Electronic Supplementary Information

Modulating sensitivity and detection mechanism with spacer chain length: a new series of fluorescent turn on chemodosimeters and a chemosensor for Pb^{2+} based on rhodamine-quinoline conjugates

Manisha Devi,[a] Abhimanew Dhir,[a] Chullikkattil P. Pradeep[a*]

School of Basic Science, Indian Institute of Technology Mandi, Kamand-175 005, Himachal Pradesh, India.
Fax: +91 1905 267009; Tel: +91 1905 267045; E-mail: pradeep@iitmandi.ac.in

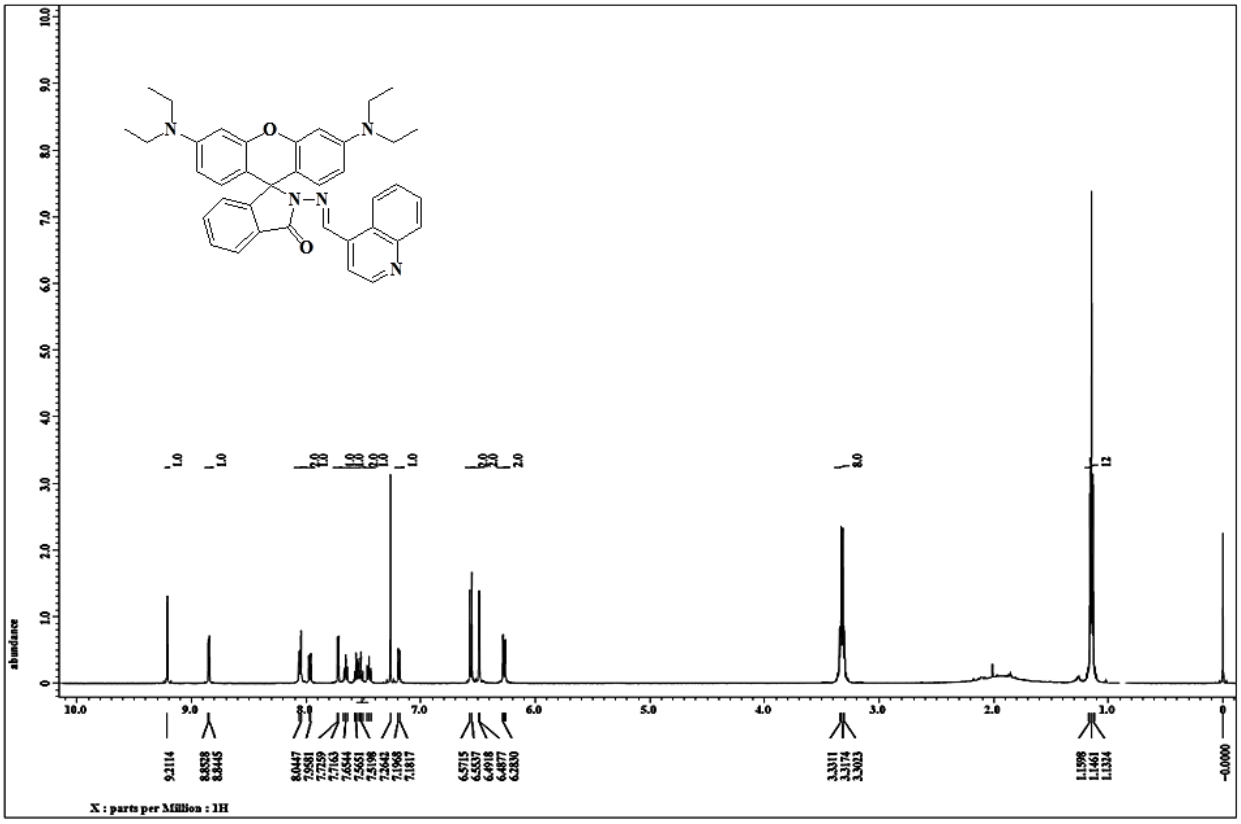

Fig. S1 ^{1}H NMR spectrum of **RHQ-1**.

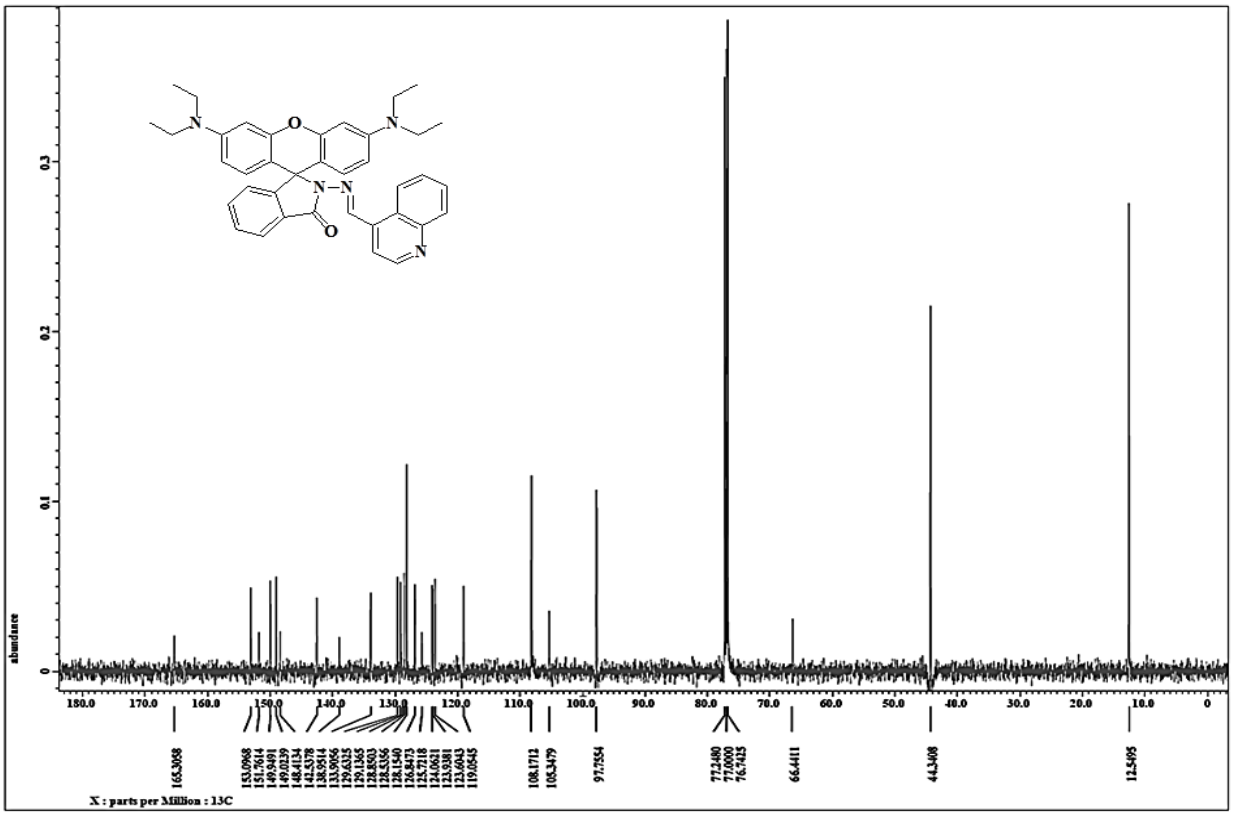

Fig. S2 ^{13}C NMR spectrum of **RHQ-1**.

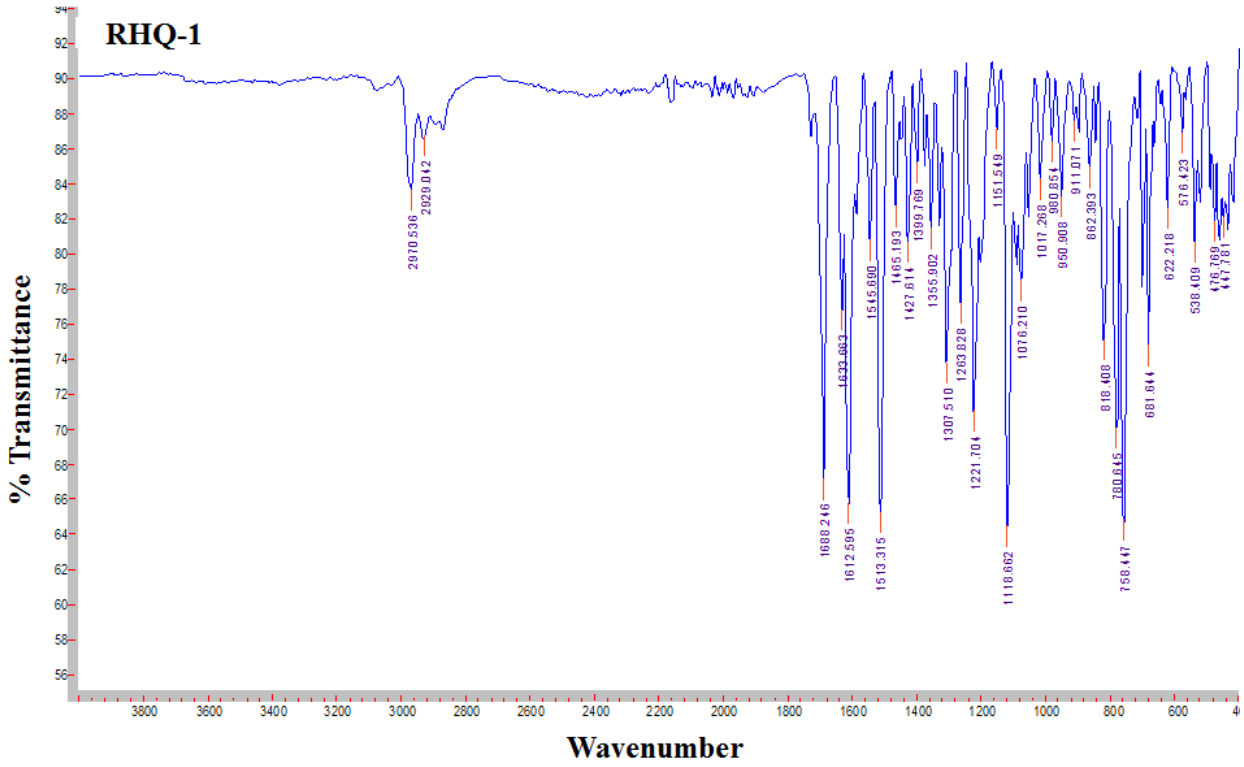

Fig. S3 IR spectrum of **RHQ- 1**.

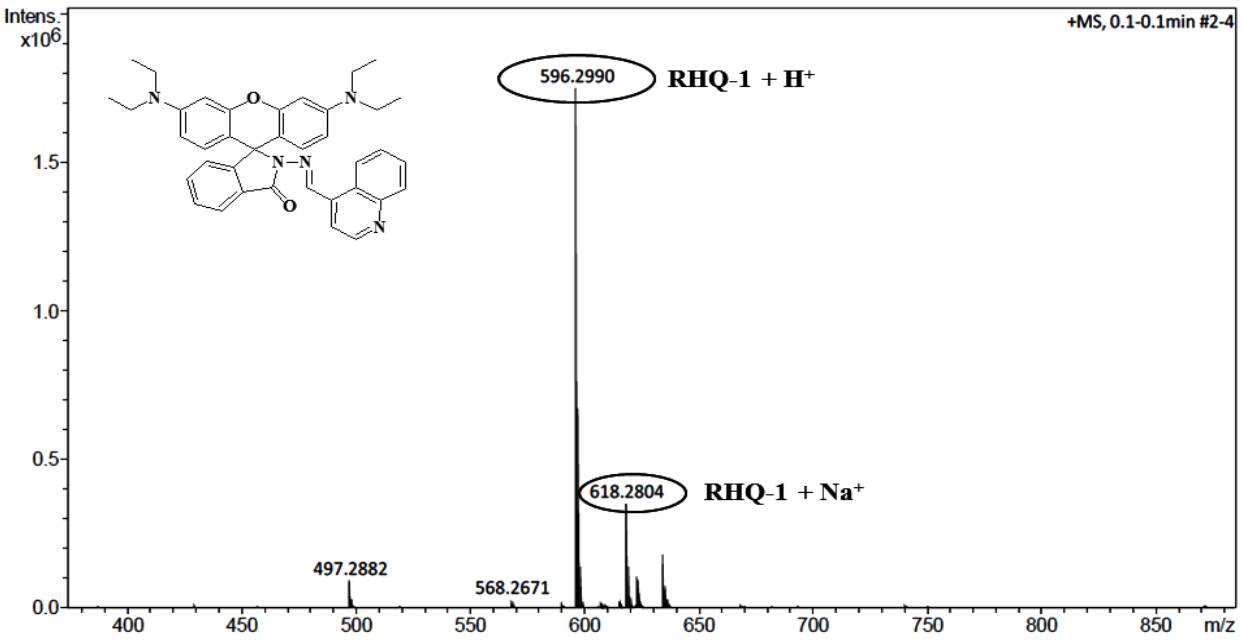

Fig. S4 Mass spectrum of **RHQ-1**.

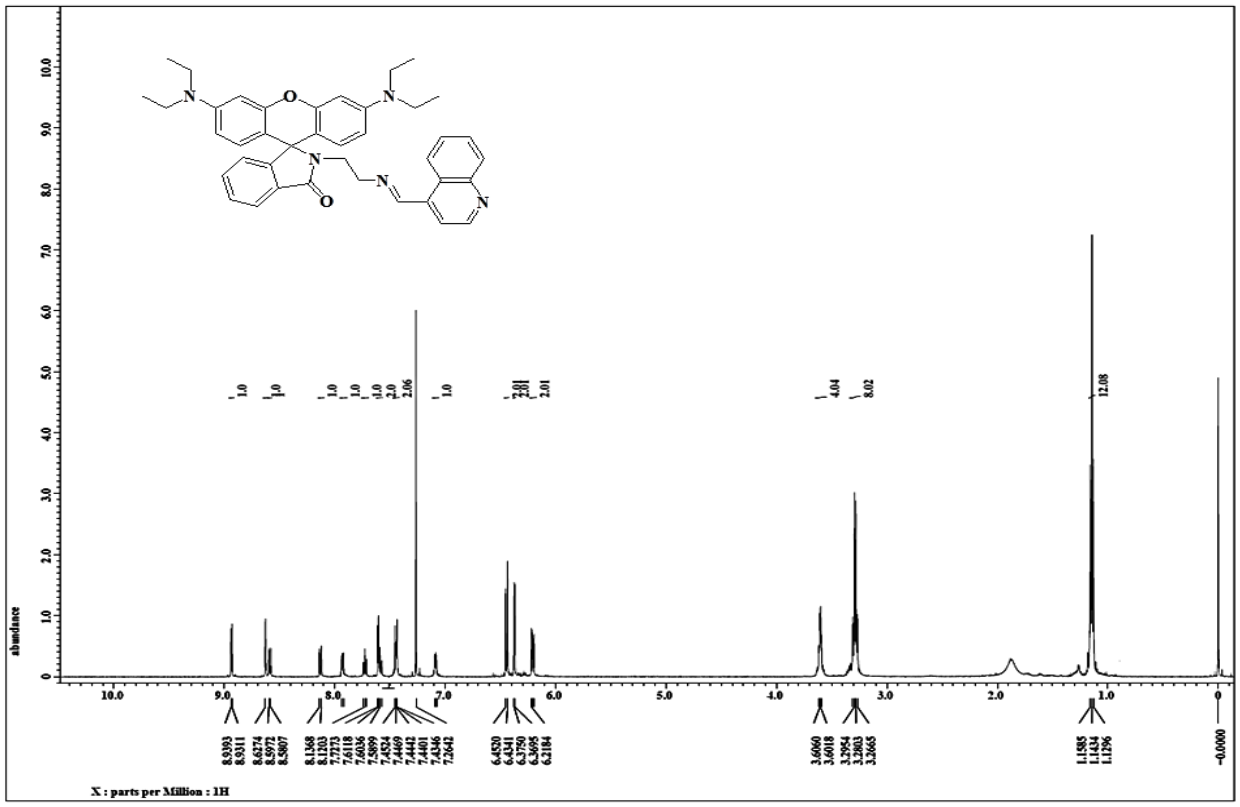

Fig. S5 ^{1}H NMR spectrum of **RHQ-2**.

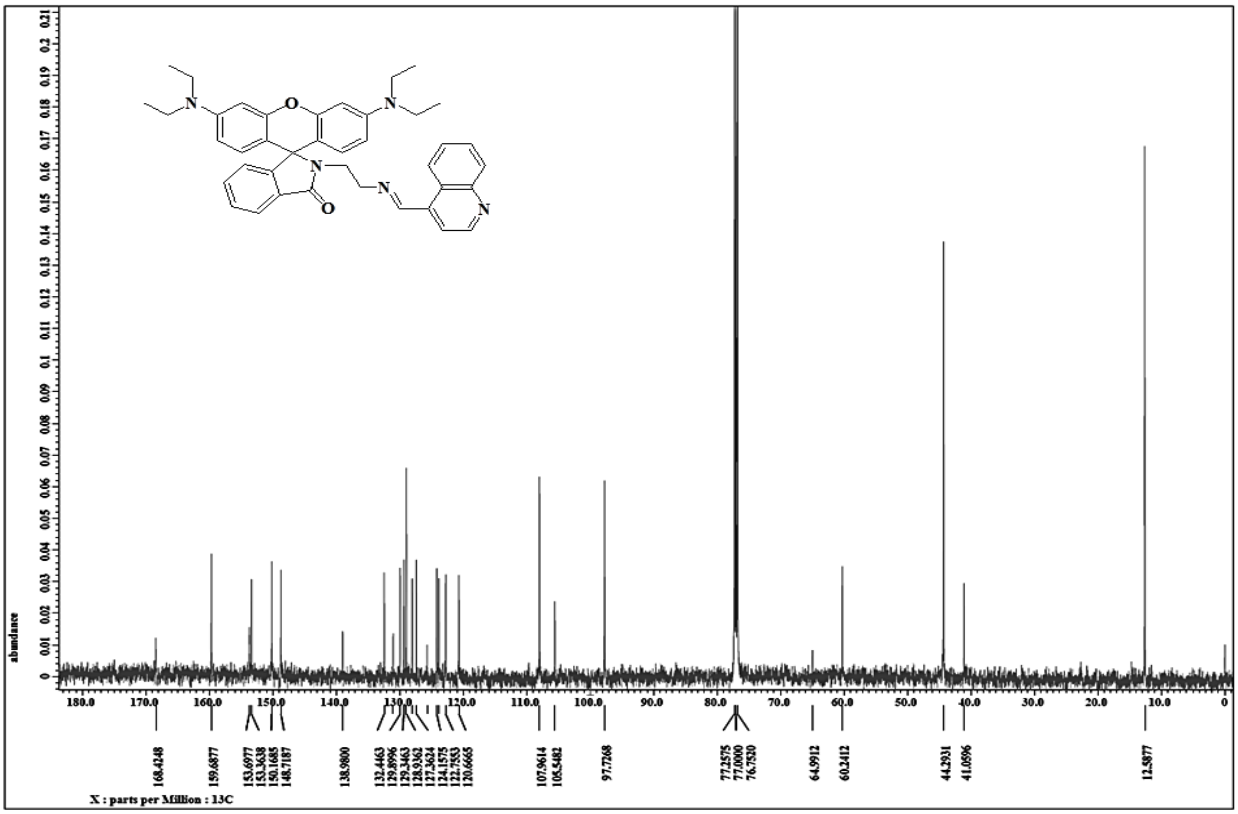

Fig. S6 ^{13}C NMR spectrum of **RHQ-2**.

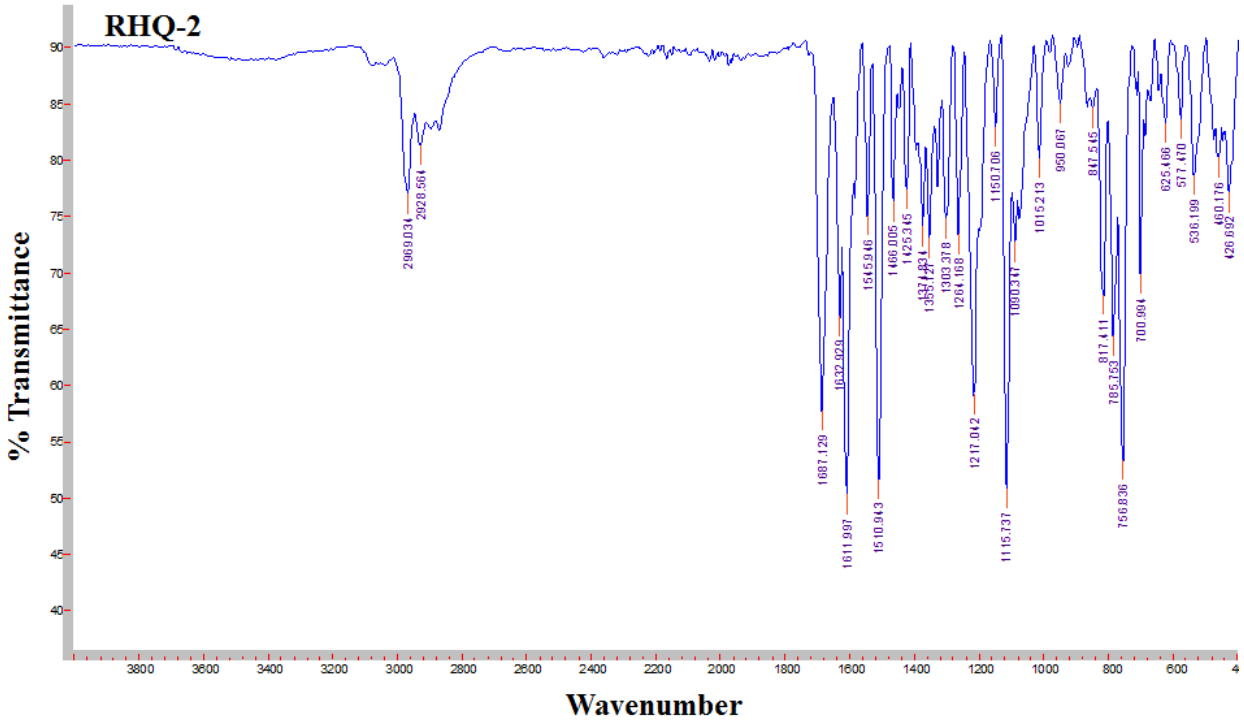

Fig. S7 IR spectrum of **RHQ-2**.

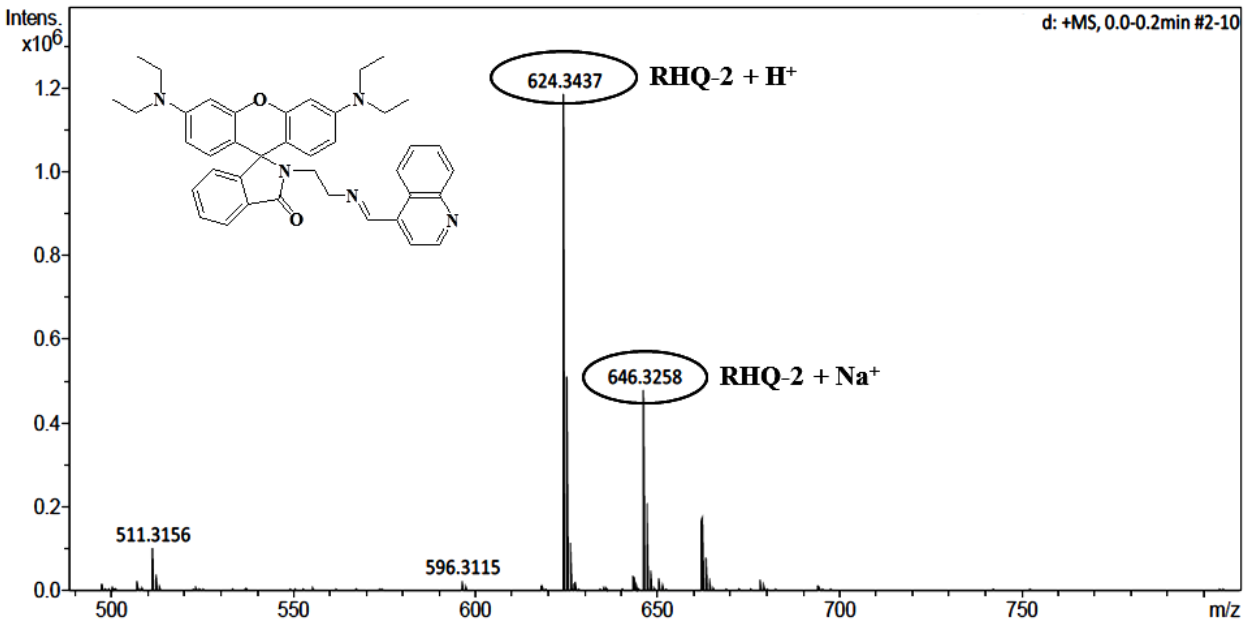

Fig. S8 Mass spectrum of **RHQ-2**.

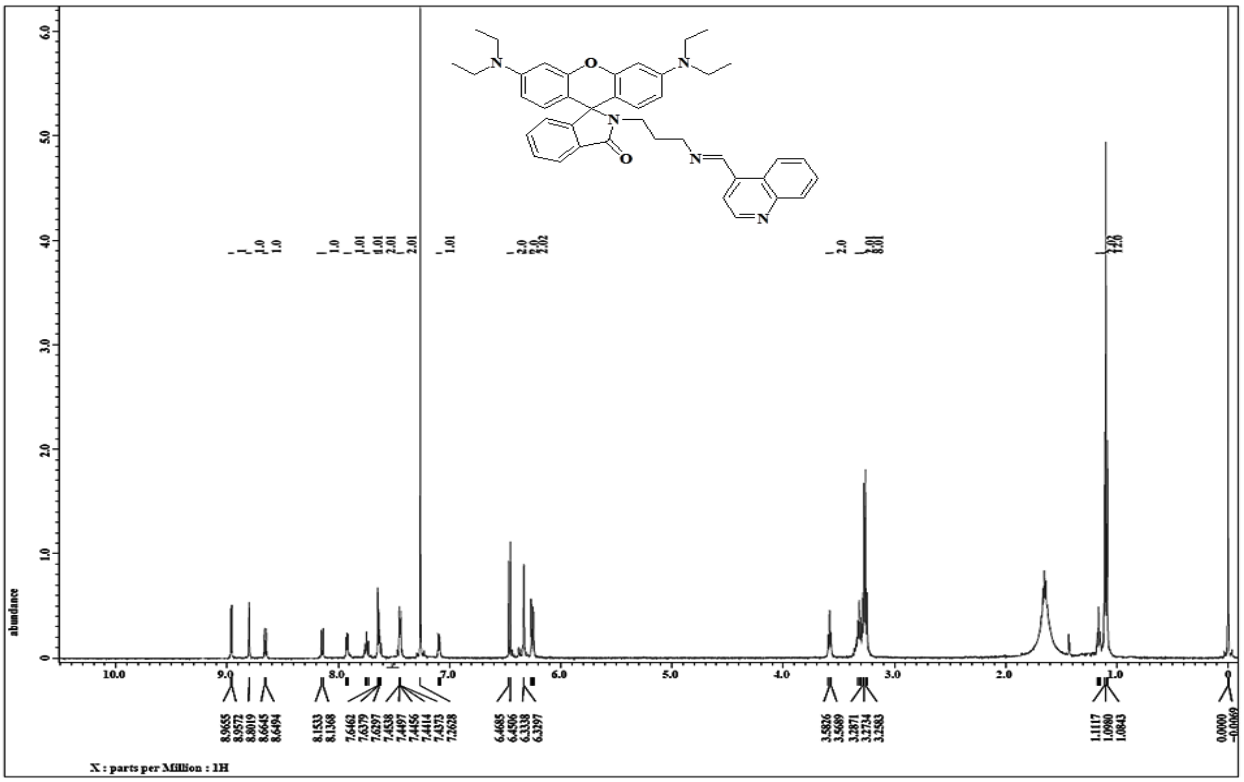

Fig. S9 ^{1}H NMR spectrum of **RHQ-3**.

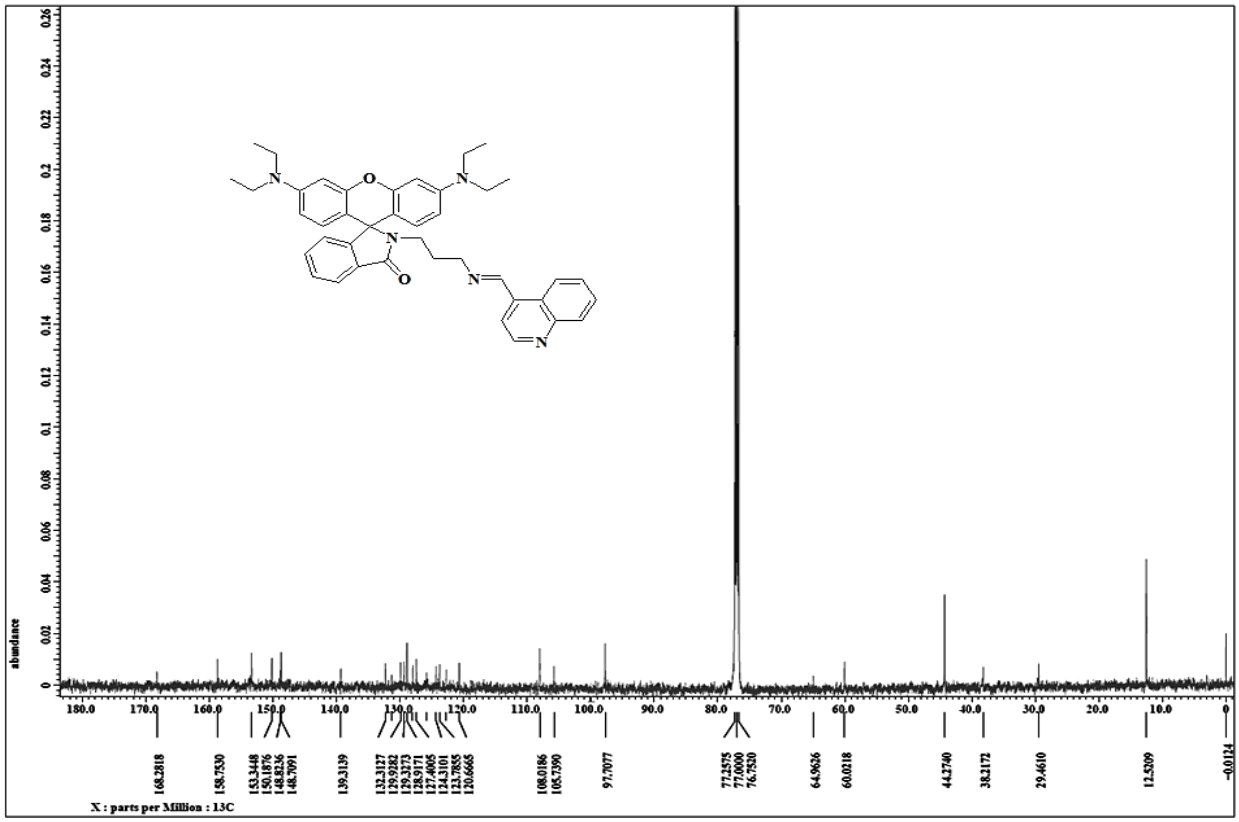

Fig. S10 ^{13}C NMR spectrum of **RHQ-3**.

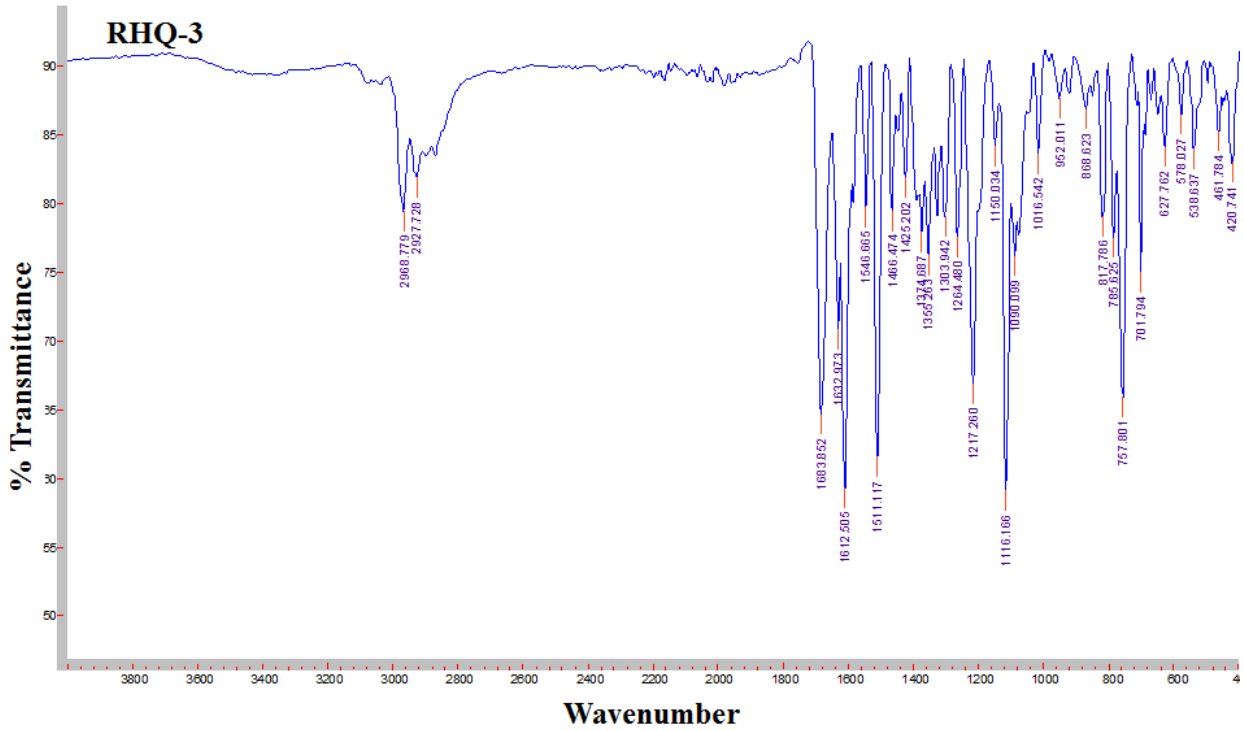

Fig. S11 IR spectrum of **RHQ-3**.

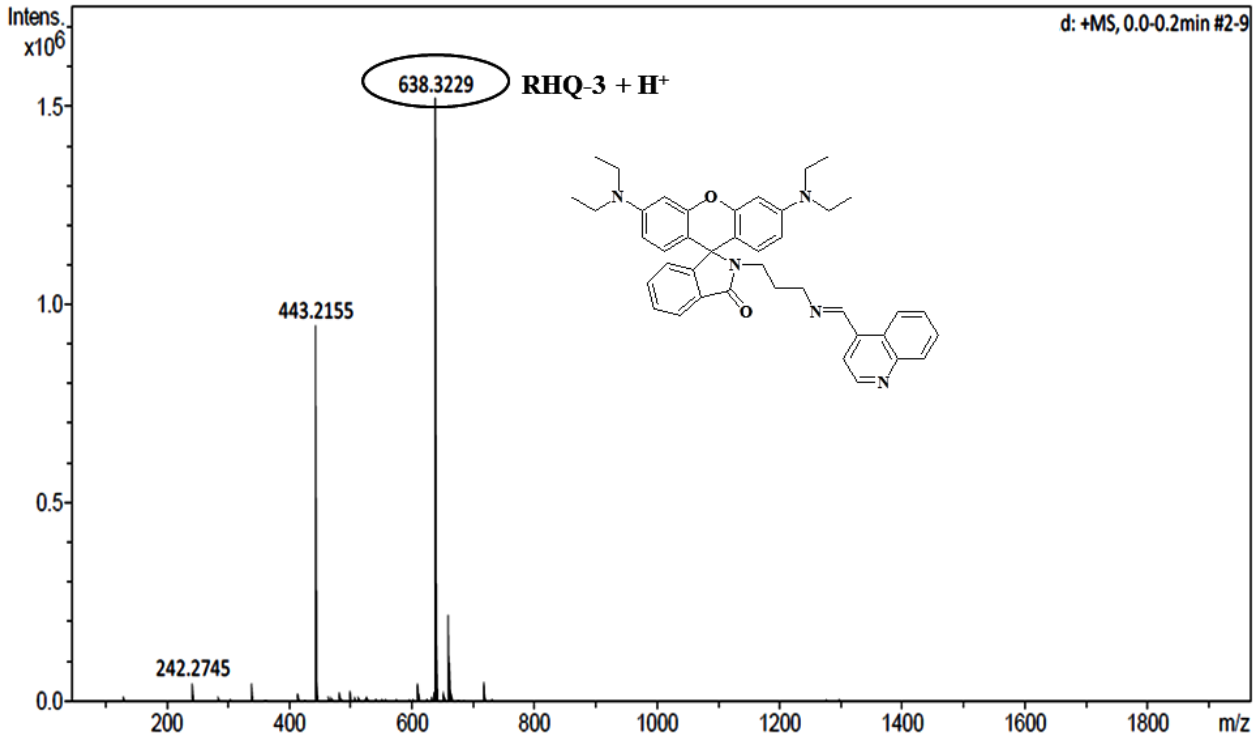

Fig. S12 Mass spectrum of **RHQ-3**.

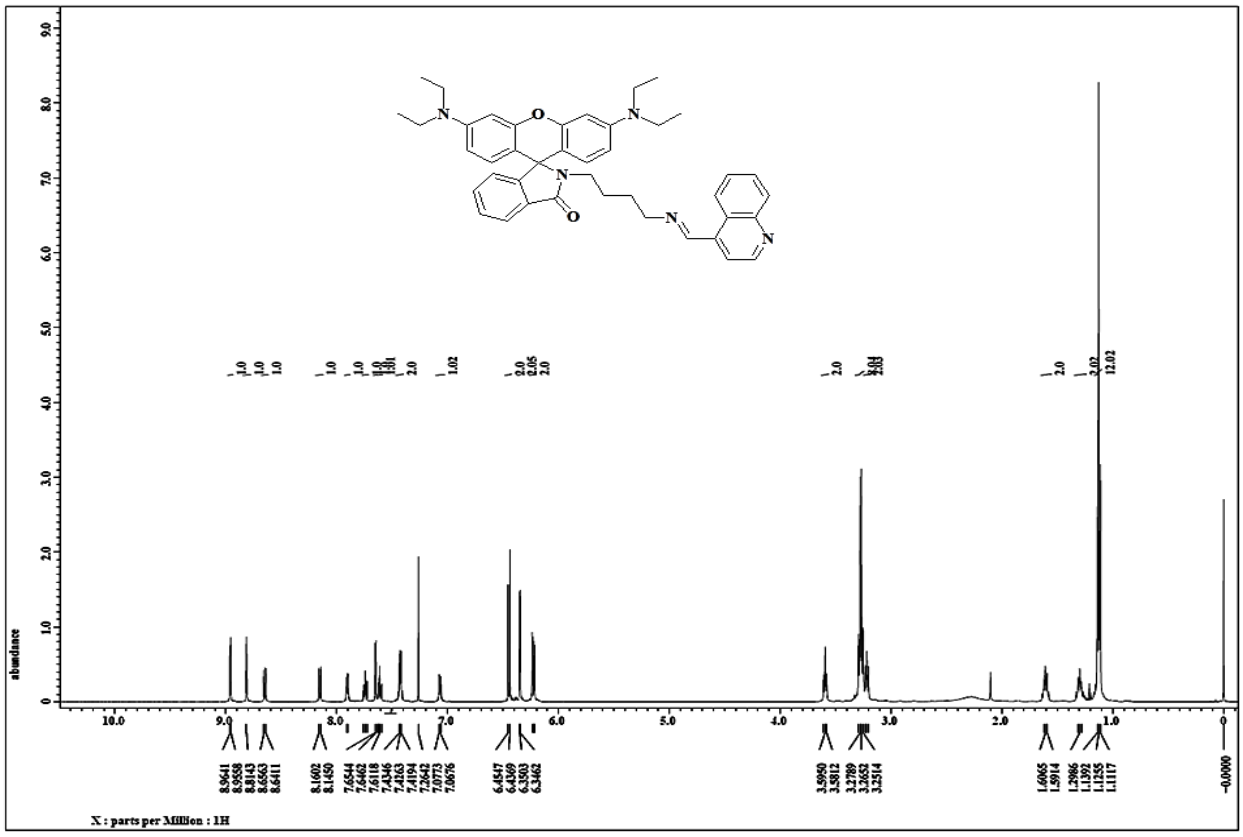

Fig. S13 ^{1}H NMR spectrum of **RHQ-4**.

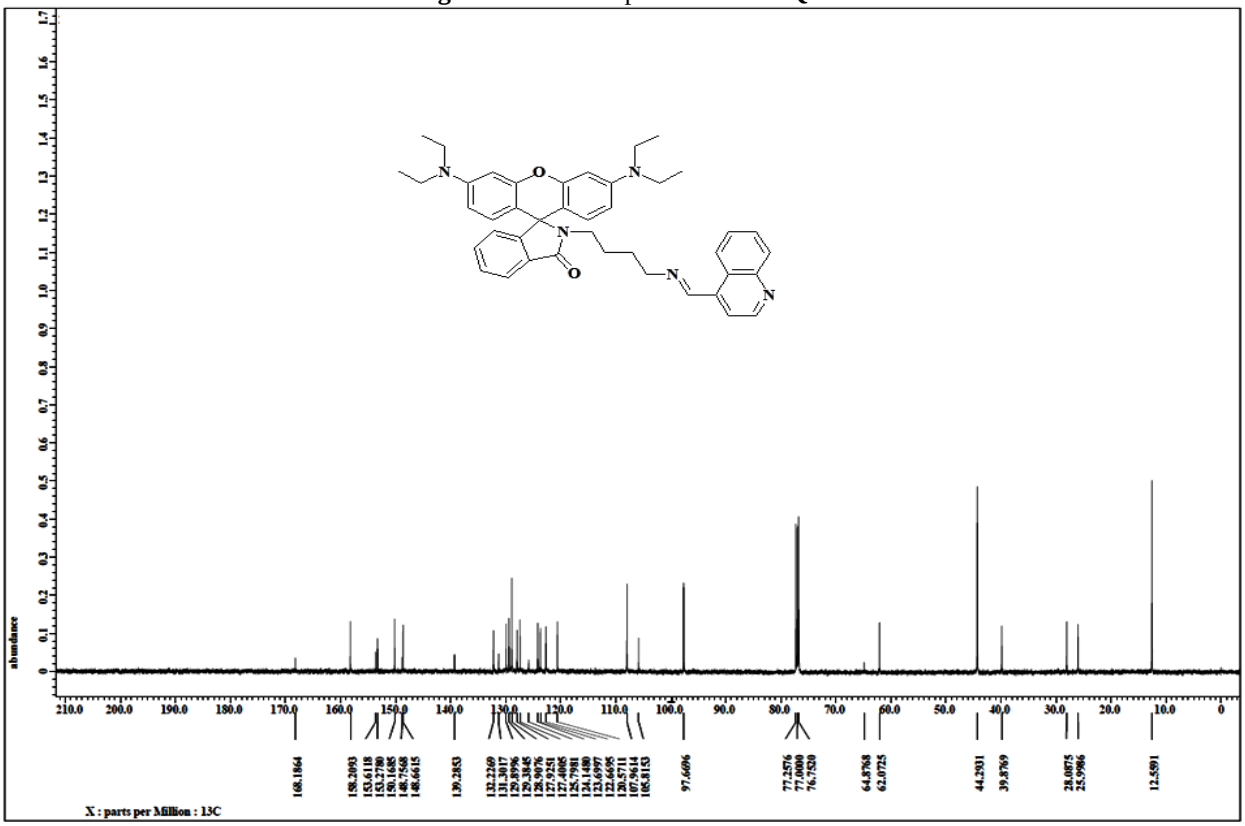

Fig. S14 ^{13}C NMR spectrum of **RHQ-4**.

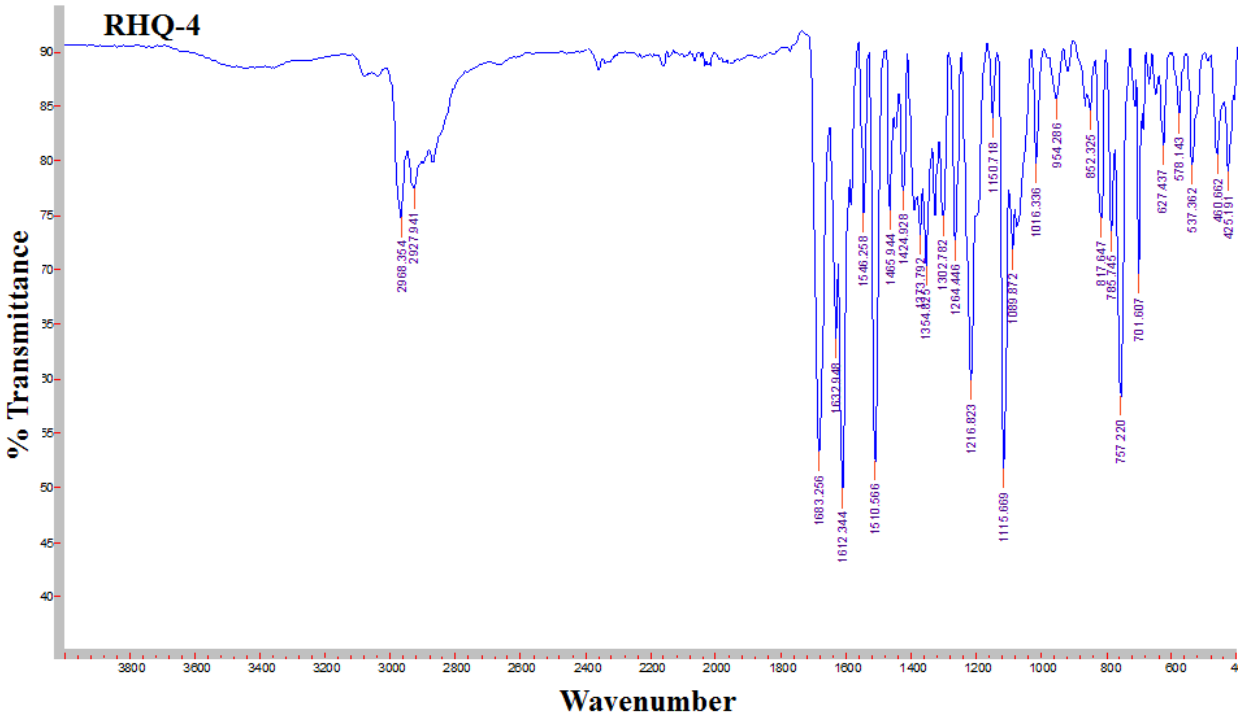

Fig. S15 IR spectrum of **RHQ-4**.

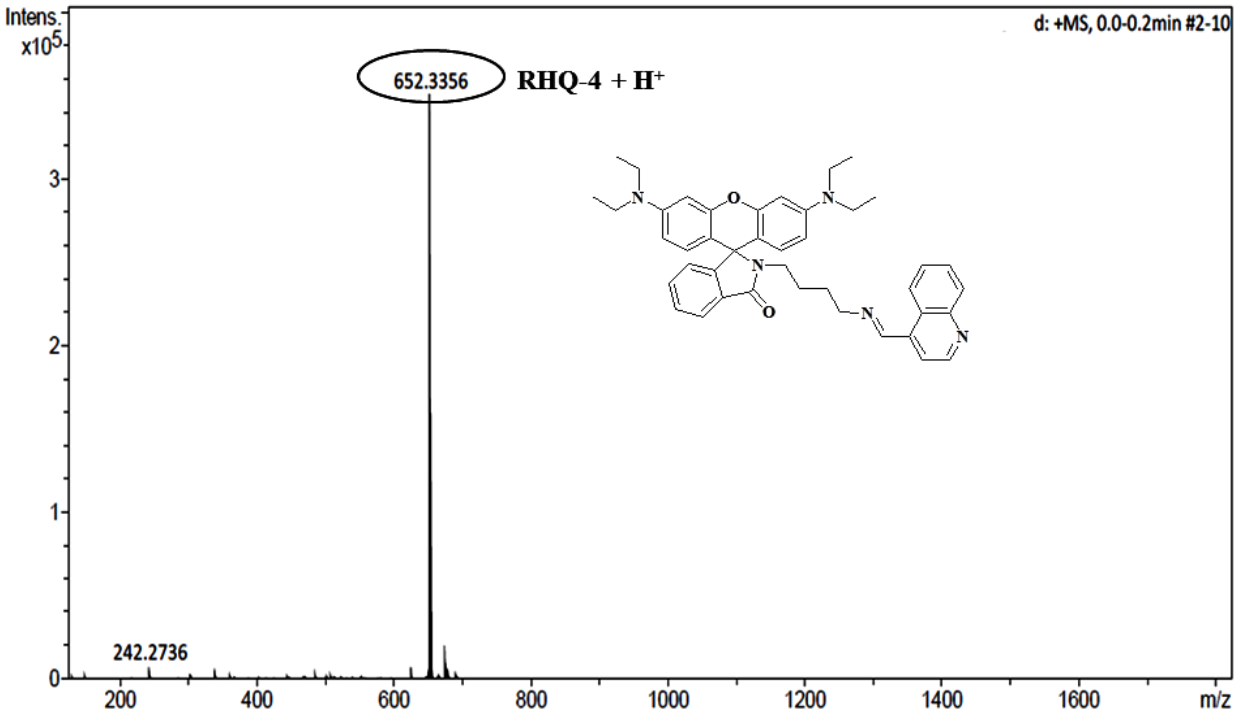

Fig. S16 Mass spectrum of **RHQ-4**.

Fluorescence studies

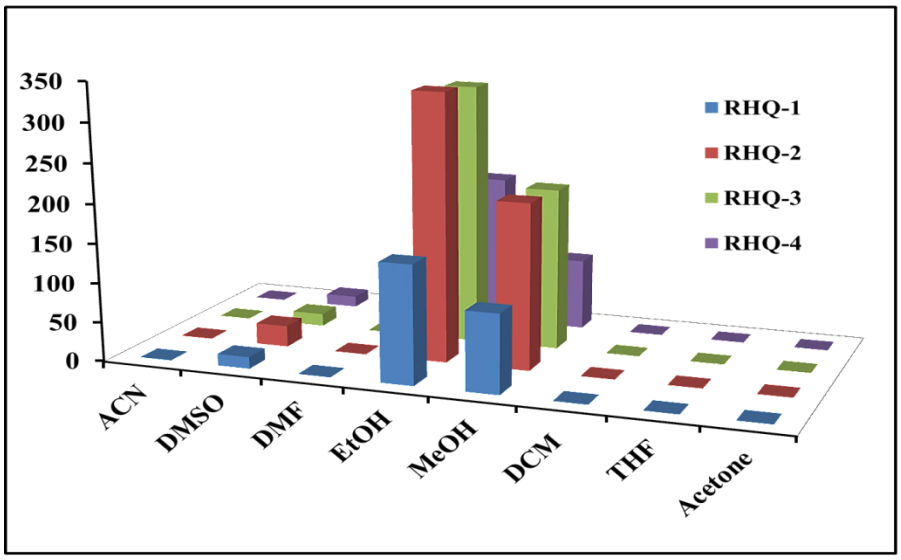

Fig. S17 Fluorescence responses of **RHQs 1-4** (1×10^{-5} M) in different solvents, λ_{ex} = 530 nm.

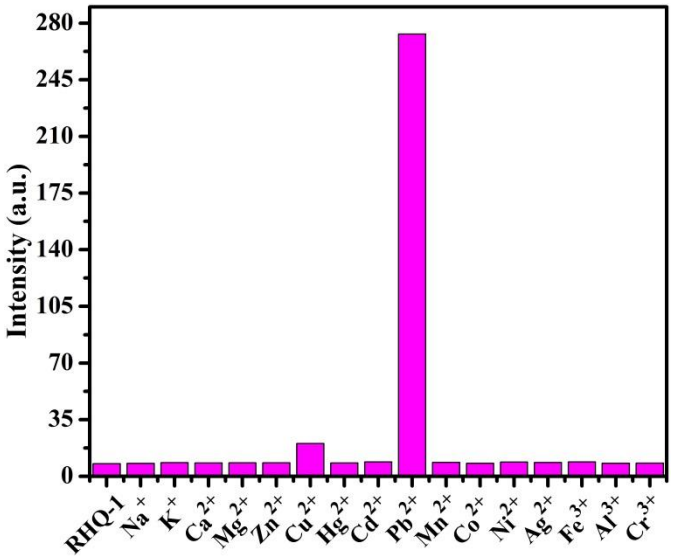

Fig. S18 Comparison of the fluorescence intensity of **RHQ-1** (1×10^{-5} M) upon addition of 0.061 equiv. of various metal ions in CH_3CN:H_2O (9.5:0.5 %, *v*/*v*).

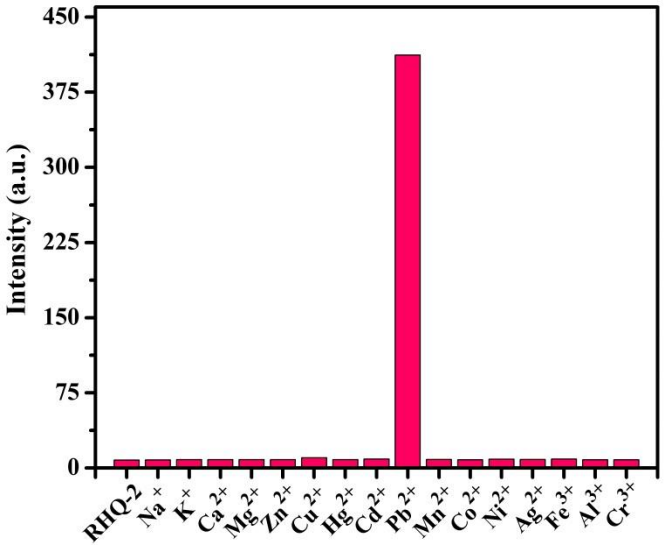

Fig. S19 Comparison of the fluorescence intensity of **RHQ-2** (1×10^{-5} M) upon addition of 0.043 equiv. of various metal ions in CH_3CN:H_2O (9.5:0.5 %, *v*/*v*).

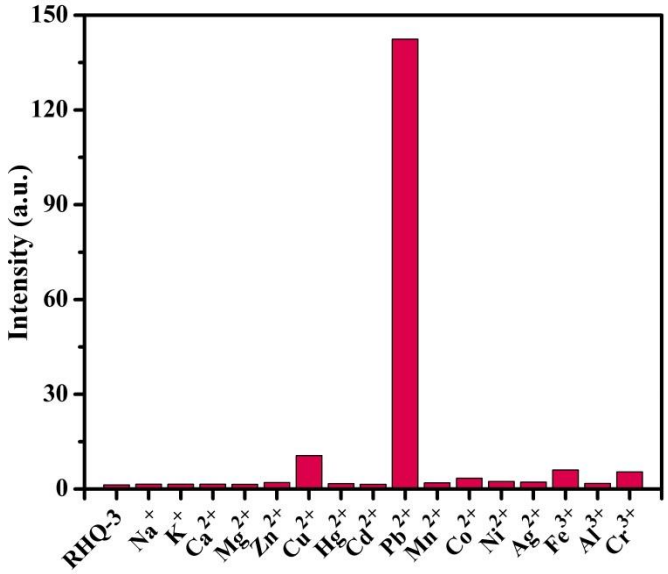

Fig. S20 Comparison of the fluorescence intensity of **RHQ-3** (1×10^{-5} M) upon addition of 0.020 equiv. of various metal ions in CH_3CN:H_2O (9.5:0.5 %, *v*/*v*).

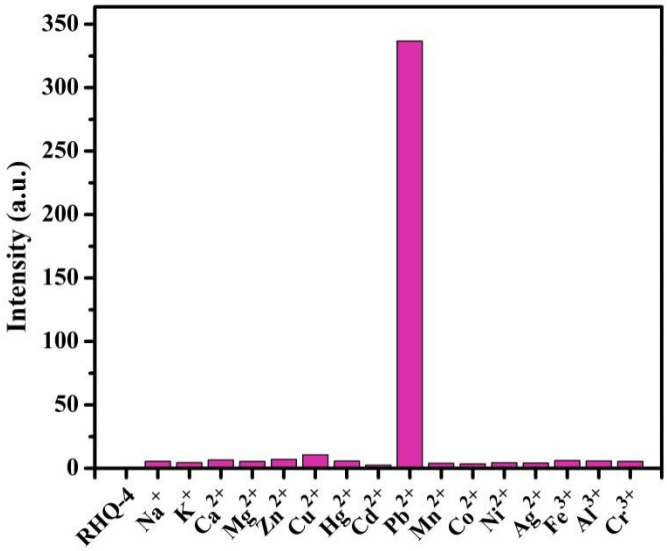

Fig. S21 Comparison of the fluorescence intensity of **RHQ-4** (1×10^{-5} M) upon addition of 3.04 equiv. of various metal ions in CH_3CN:H_2O (9.5:0.5 %, *v*/*v*).

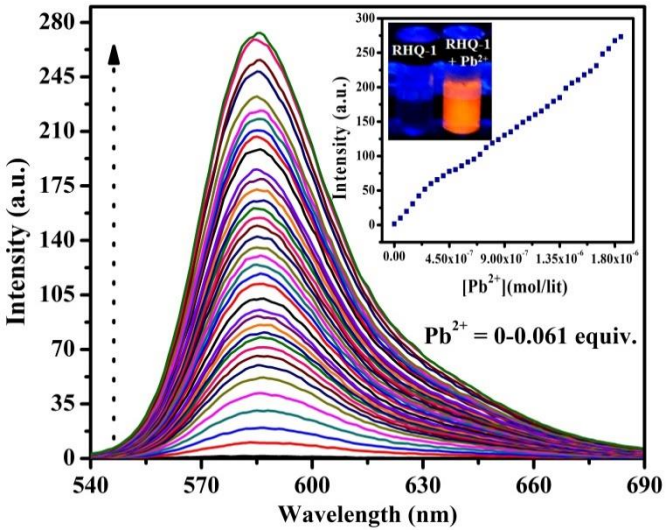

Fig. S22 Fluorescence spectra of **RHQ-1** (1×10^{-5} M) upon addition of 0.061 equiv. of Pb^{2+} in CH_3CN:H_2O (9.5:0.5 %, *v*/*v*).

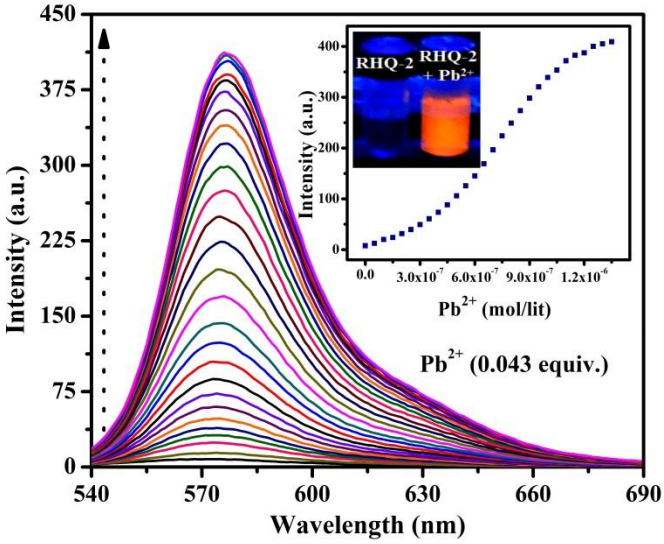

Fig. S23 Fluorescence spectra of **RHQ-2** (1×10^{-5} M) upon addition of 0.043 equiv. of Pb^{2+} in CH_3CN: H_2O (9.5:0.5 %, *v*/*v*).

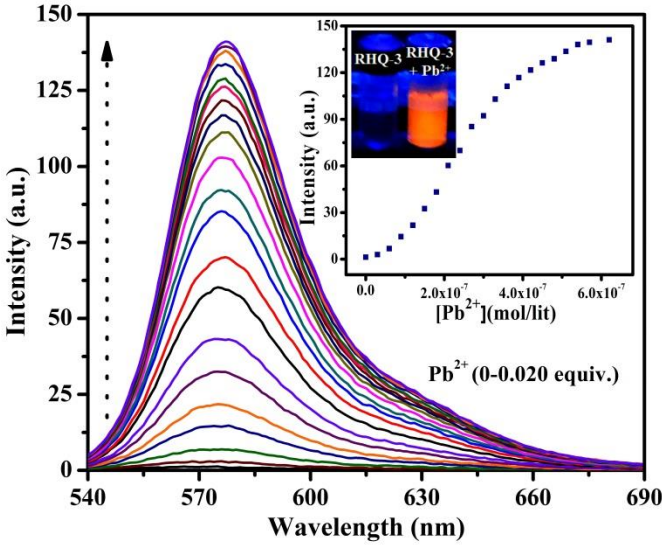

Fig. S24 Fluorescence spectra of **RHQ-3** (1×10^{-5} M) upon addition of 0.020 equiv. of Pb^{2+} in CH_3CN:H_2O (9.5:0.5 %, *v*/*v*).

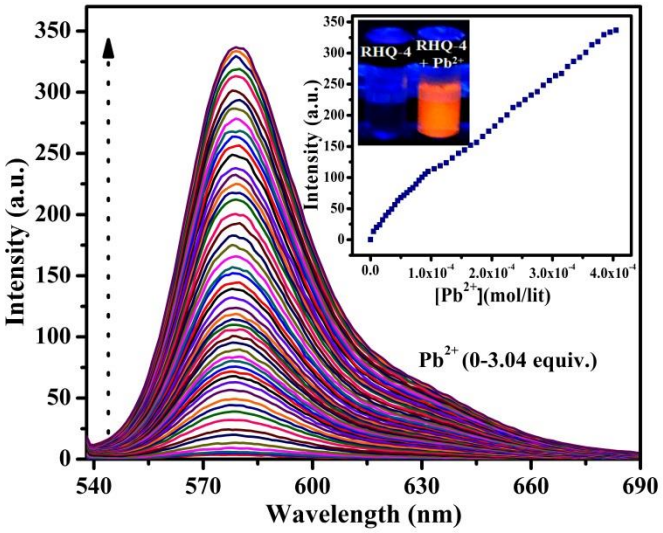

Fig. S25 Fluorescence spectra of **RHQ-4** (1×10^{-5} M) upon addition of 3.04 equiv. of Pb^{2+} in CH_3CN:H_2O (9.5:0.5 %, *v*/*v*).

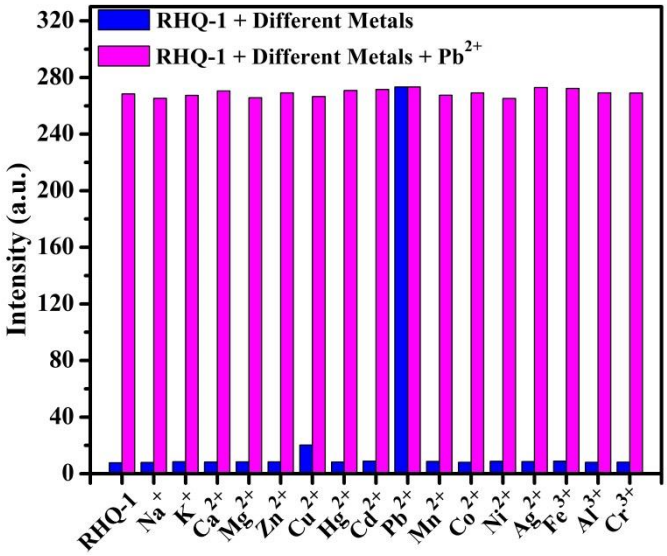

Fig. S26 Fluorescence response of **RHQ-1** (1×10^{-5} M) in CH_3CN:H_2O (9.5:0.5 %, *v*/*v*) upon addition of 0.061 equiv. of respective metal ions (blue bars), followed by addition of 0.061 equiv. of Pb^{2+} (pink bars). λ_{ex} = 530 nm.

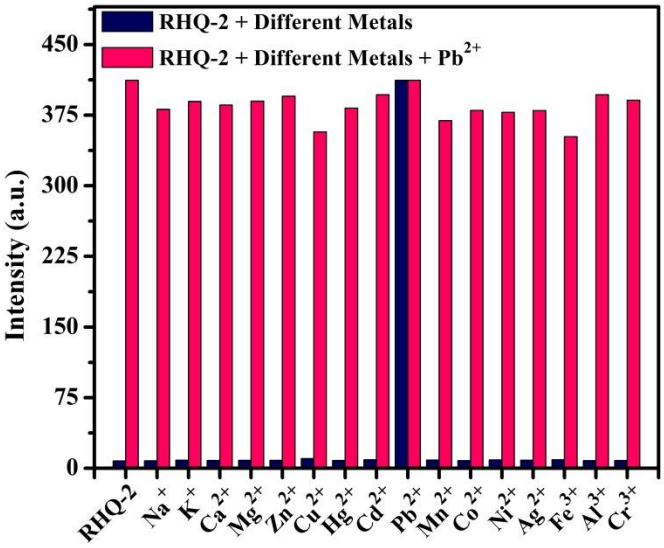

Fig. S27 Fluorescence response of **RHQ-2** (1×10^{-5} M) in CH_3CN:H_2O (9.5:0.5 %, *v*/*v*) upon addition of 0.043 equiv. of respective metal ions (blue bars), followed by addition of 0.043 equiv. of Pb^{2+} (pink bars). λ_{ex} = 530 nm.

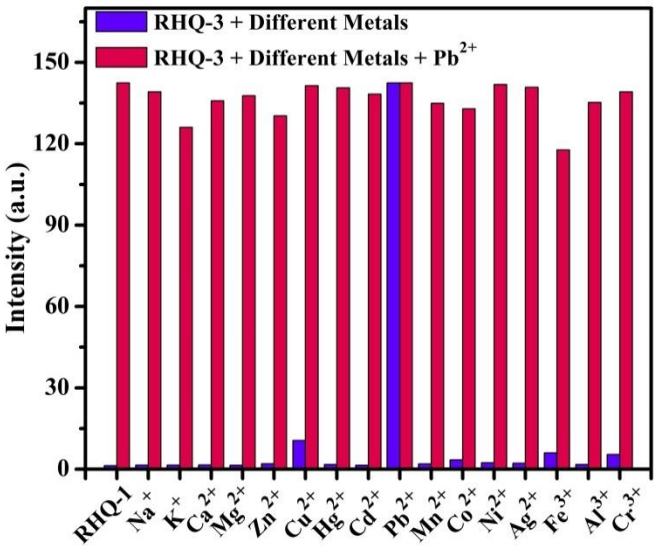

Fig. S28 Fluorescence response of **RHQ-3** (1×10^{-5} M) in CH_3CN:H_2O (9.5:0.5 %, *v*/*v*) upon addition of 0.020 equiv. of respective metal ions (blue bars), followed by addition of 0.020 equiv. of Pb^{2+} (pink bars). λ_{ex} = 530 nm.

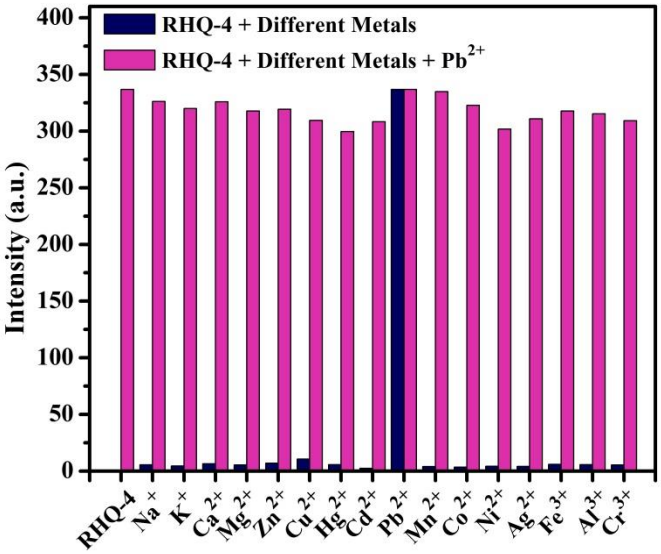

Fig. S29 Fluorescence response of **RHQ-4** (1×10^{-5} M) in CH_3CN:H_2O (9.5:0.5 %, *v*/*v*) upon addition of 3.04 equiv. of respective metal ions (blue bars), followed by addition of 3.04 equiv. of Pb^{2+} (pink bars). λ_{ex} = 530 nm.

Job's plots

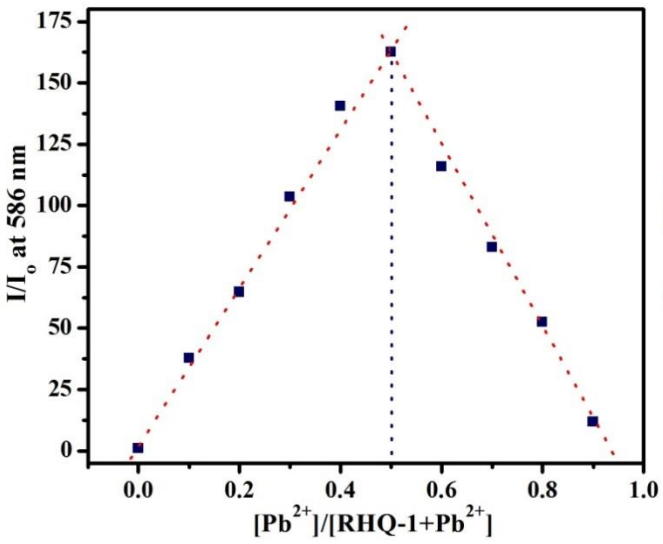

Fig. S30 Job's plot of **RHQ-1** (1×10^{-5} M) towards the detection of Pb^{2+}.

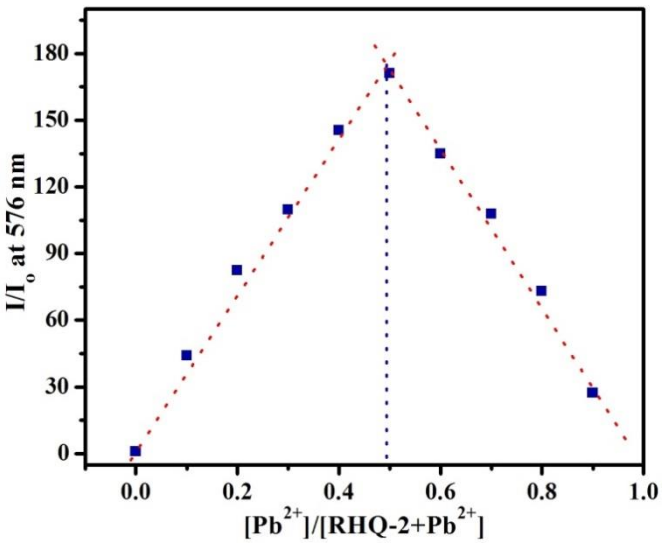

Fig. S31 Job's plot of **RHQ-2** (1×10^{-5} M) towards the detection of Pb^{2+}.

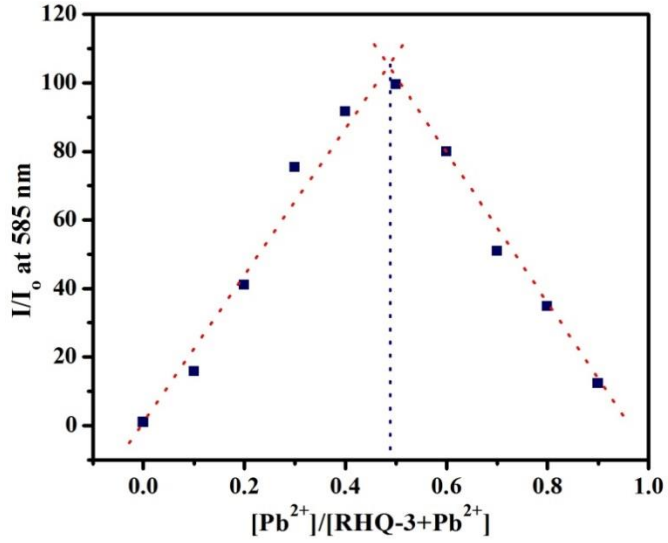

Fig. S32 Job's plot of **RHQ-3** (1×10^{-5} M) towards the detection of Pb^{2+}.

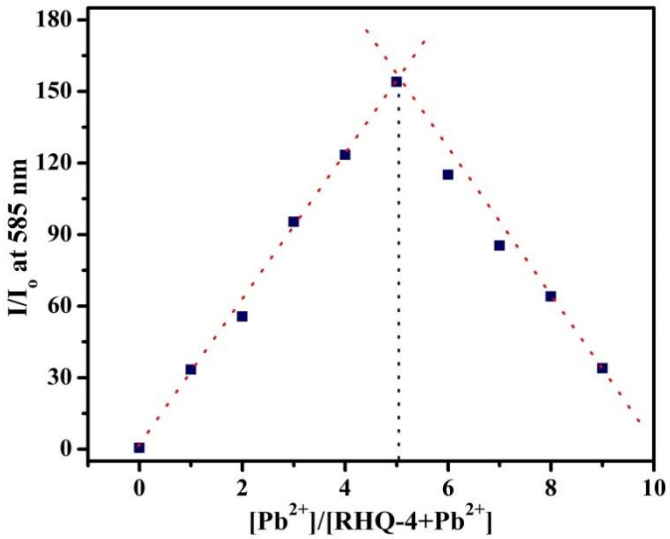

Fig. S33 Job's plot of **RHQ-4** (1×10^{-5} M) towards the detection of Pb^{2+}.

Binding constants

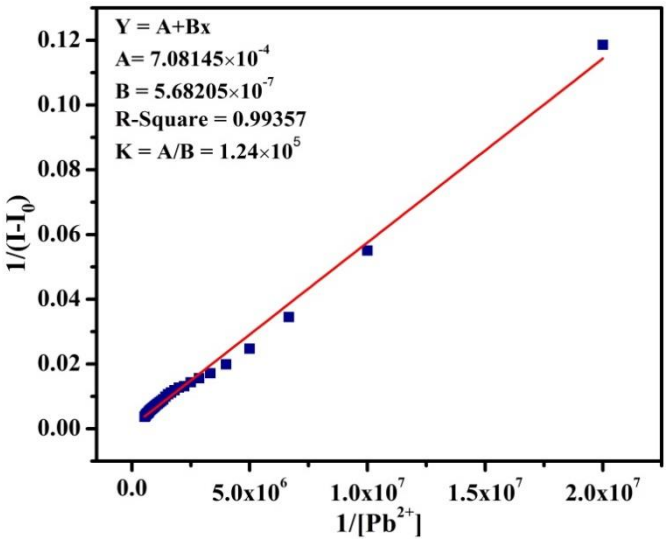

Fig. S34 Binding constant of **RHQ-1** (1×10^{-5} M) towards Pb^{2+}.

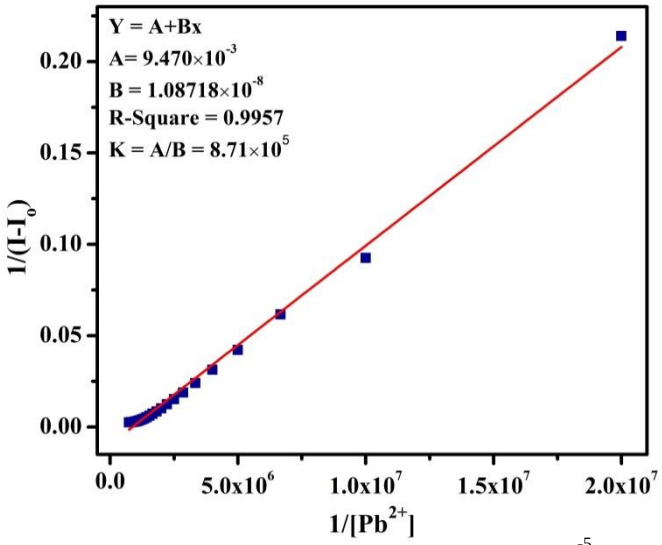

Fig. S35 Binding constant of **RHQ-2** (1×10^{-5} M) towards Pb^{2+}.

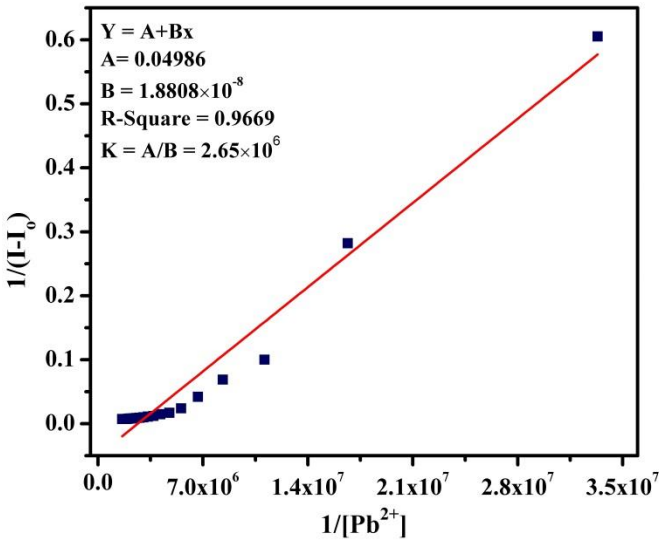

Fig. S36 Binding constant of **RHQ-3** (1×10^{-5} M) towards Pb^{2+}.

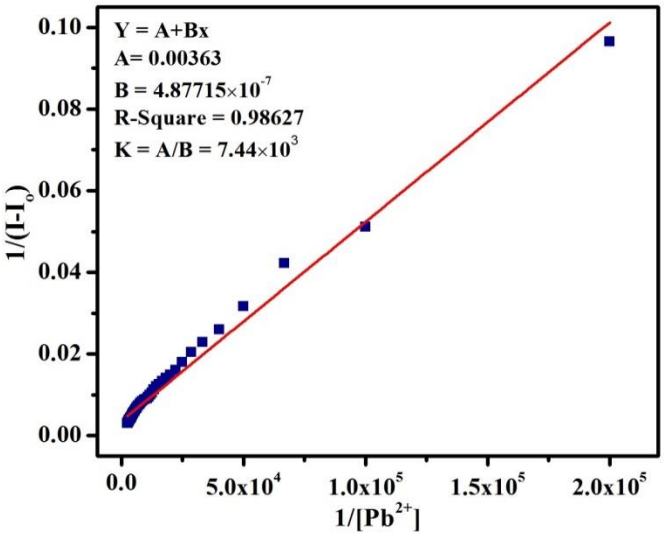

Fig. S37 Binding constant of **RHQ-4** (1×10^{-5} M) towards Pb^{2+}.

Detection limits

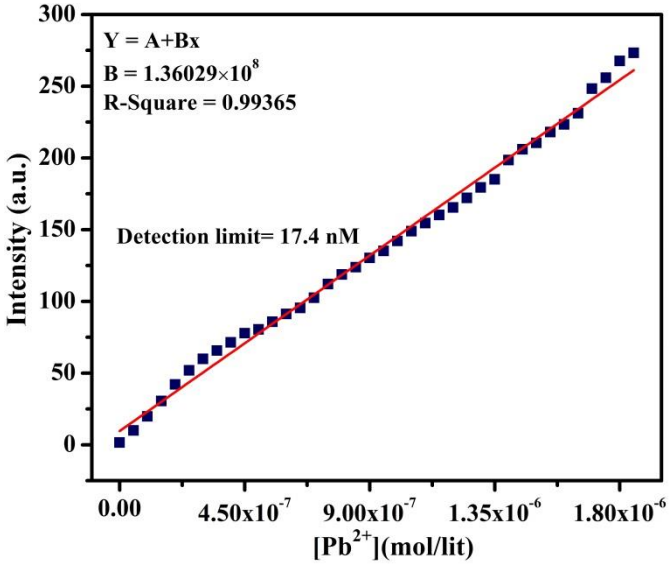

Fig. S38 Detection limit of **RHQ-1** (1×10^{-5} M) towards the detection of Pb^{2+}.

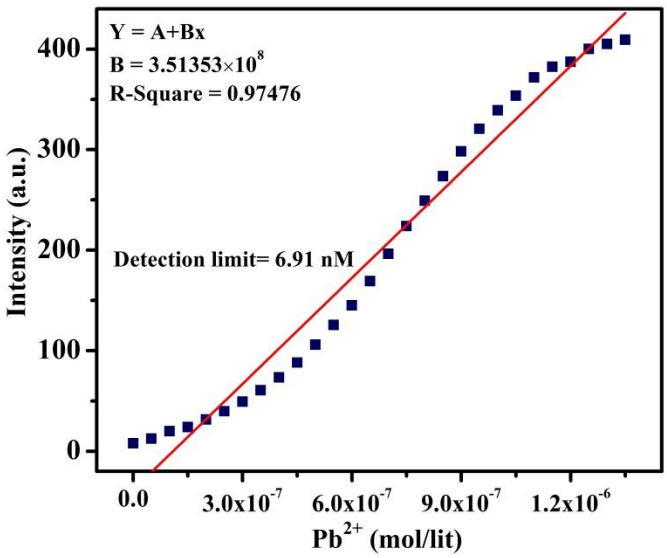

Fig. S39 Detection limit of **RHQ-2** (1×10^{-5} M) towards the detection of Pb^{2+}.

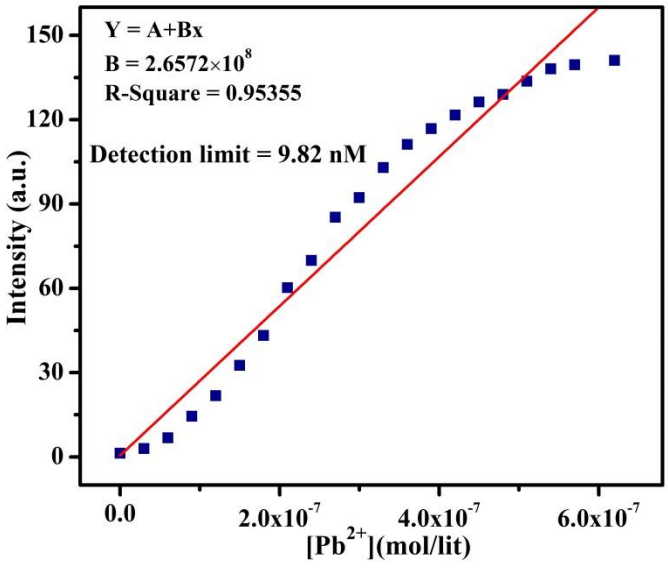

Fig. S40 Detection limit of **RHQ-3** (1×10^{-5} M) towards the detection of Pb^{2+}.

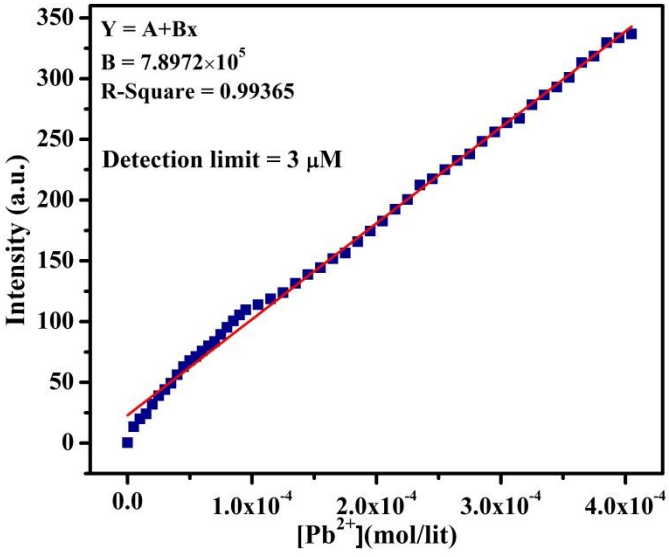

Fig. S41 Detection limit of **RHQ-4** (1×10^{-5} M) towards the detection of Pb^{2+}.

Comparison of detection limits

The detection limits of **RHQ-1, RHQ-2, RHQ-3** & **RHQ-4** towards Pb^{2+} were determined from the following equation:

$$DL=3•SD/S$$

Where SD is the standard deviation of the blank solution (**RHQ-1, RHQ-2, RHQ-3** & **RHQ-4**, 10 μM) detected for 10 times; S is the slope of the calibration curve.

S. No.	Standard Deviation	Slope	(3×Standard deviation)/Slope	Detection Limit
1.	0.71	1.36029×10^{8}	1.74×10^{-8}	17.4 nM
2.	0.81	3.51353×10^{8}	0.691×10^{-8}	6.91 nM
3.	0.87	2.6572×10^{8}	0.982×10^{-8}	9.82 nM
4.	0.79	7.8972×10^{5}	0.300×10^{-5}	3 μM

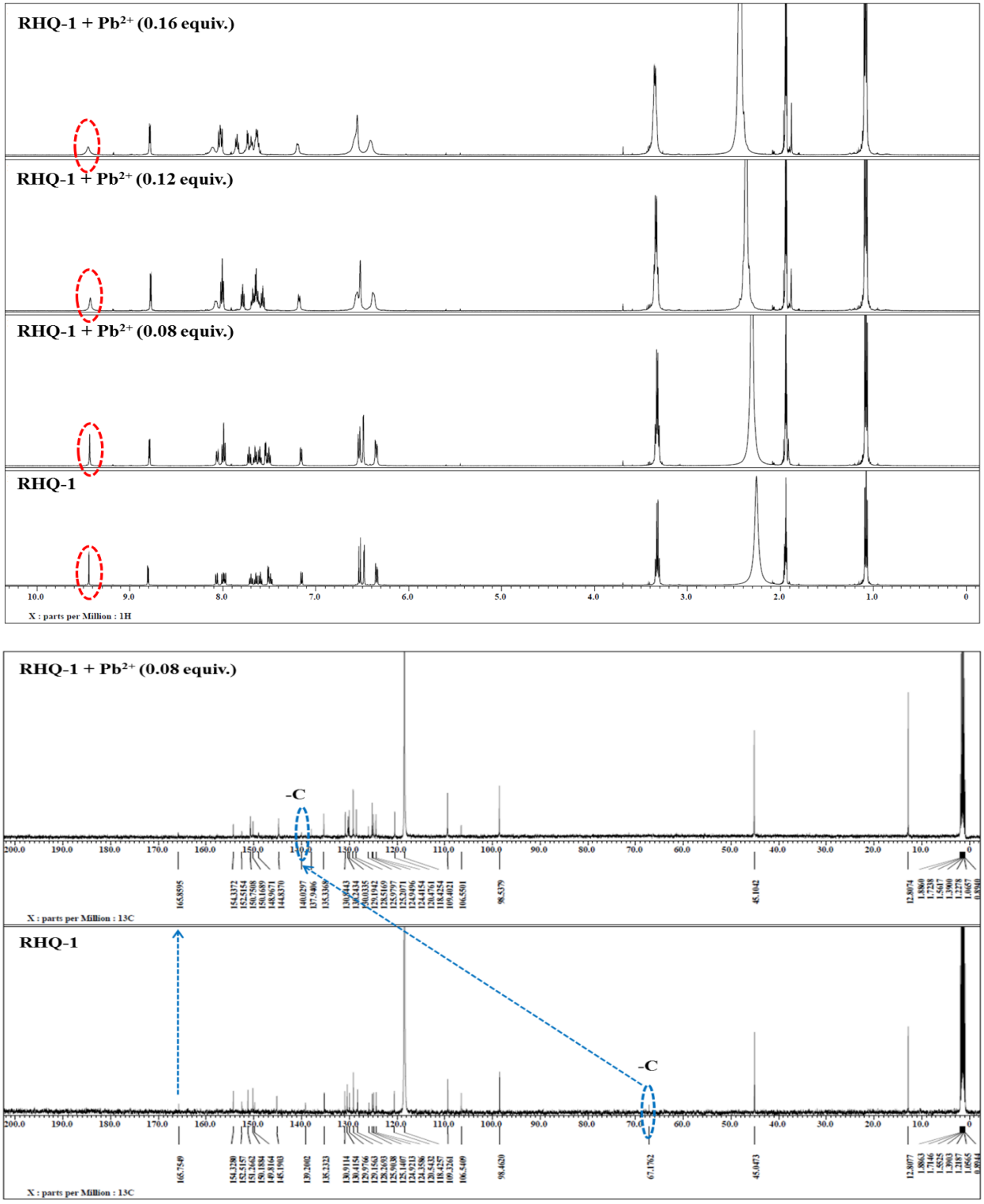

Fig. S42 ^{1}H NMR and ^{13}C NMR spectra of **RHQ-1** in CD_3CN-d_3 after addition of Pb^{2+}.

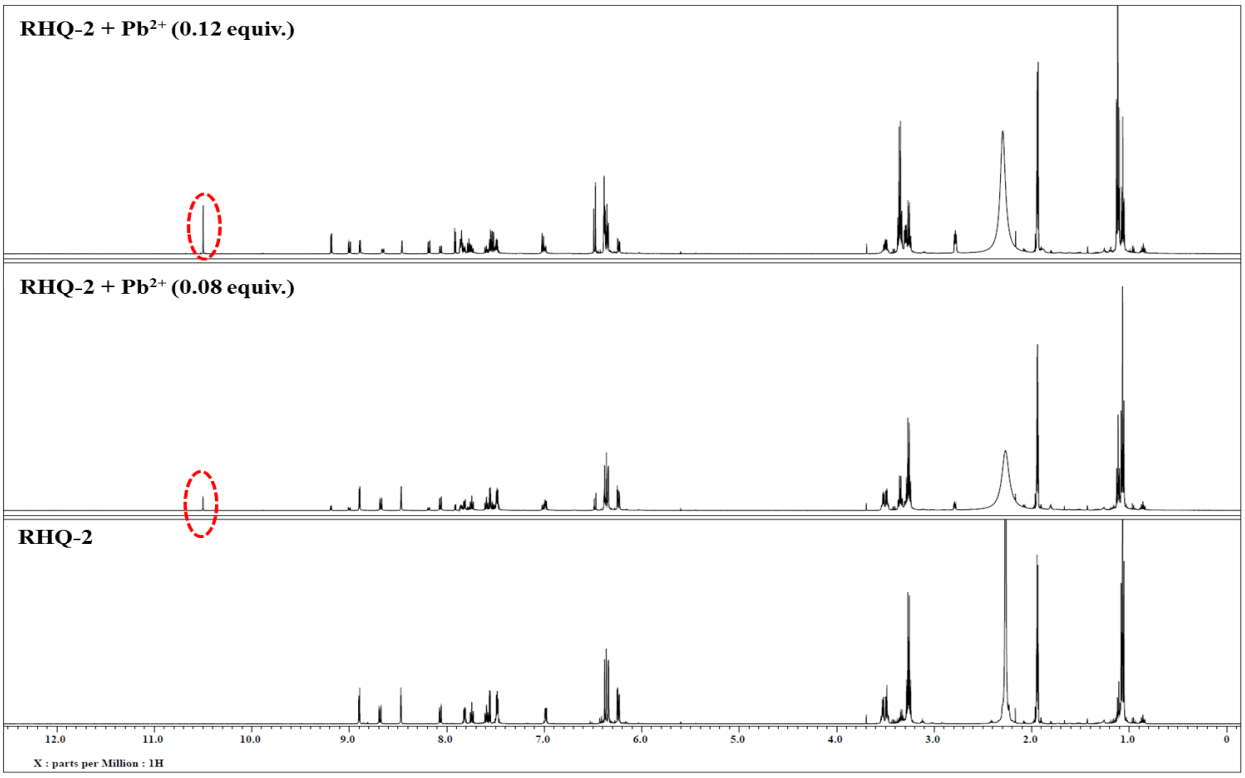

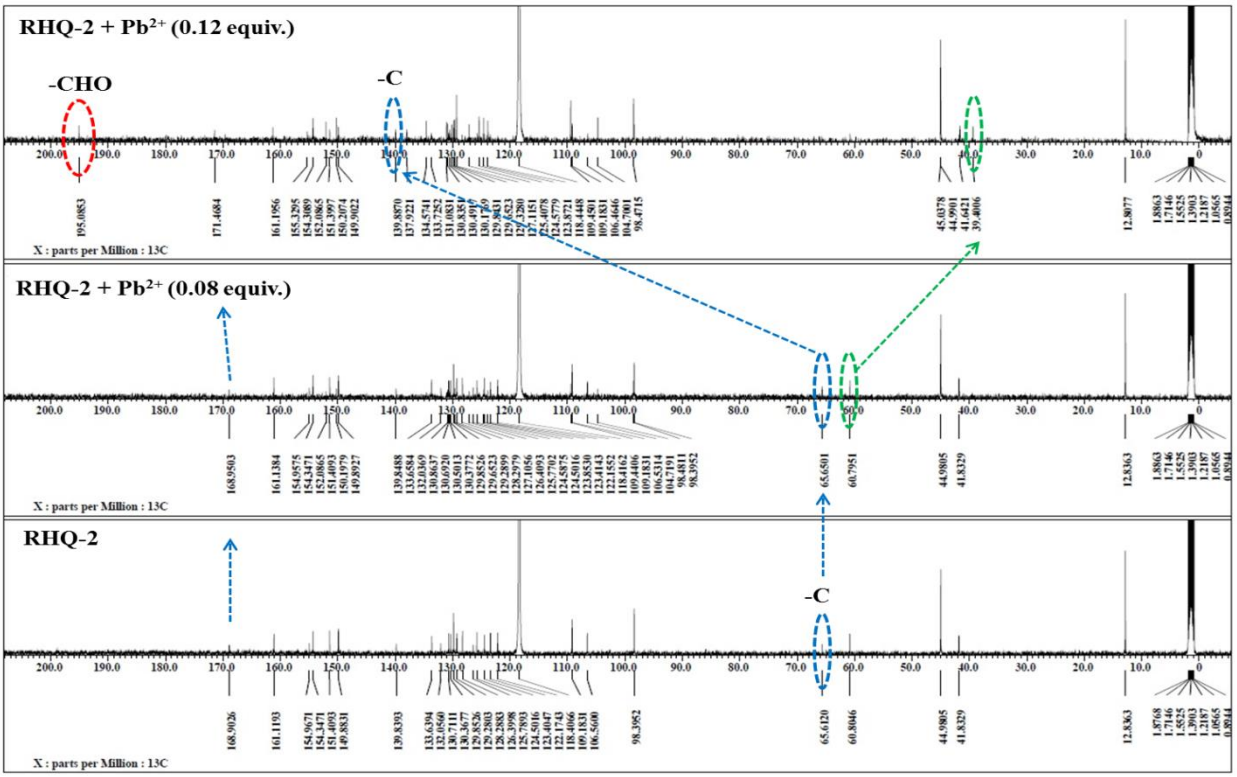

Fig. S43 ^{1}H NMR and ^{13}C NMR spectra of **RHQ-2** in CD_3CN-d_3 after addition of Pb^{2+}.

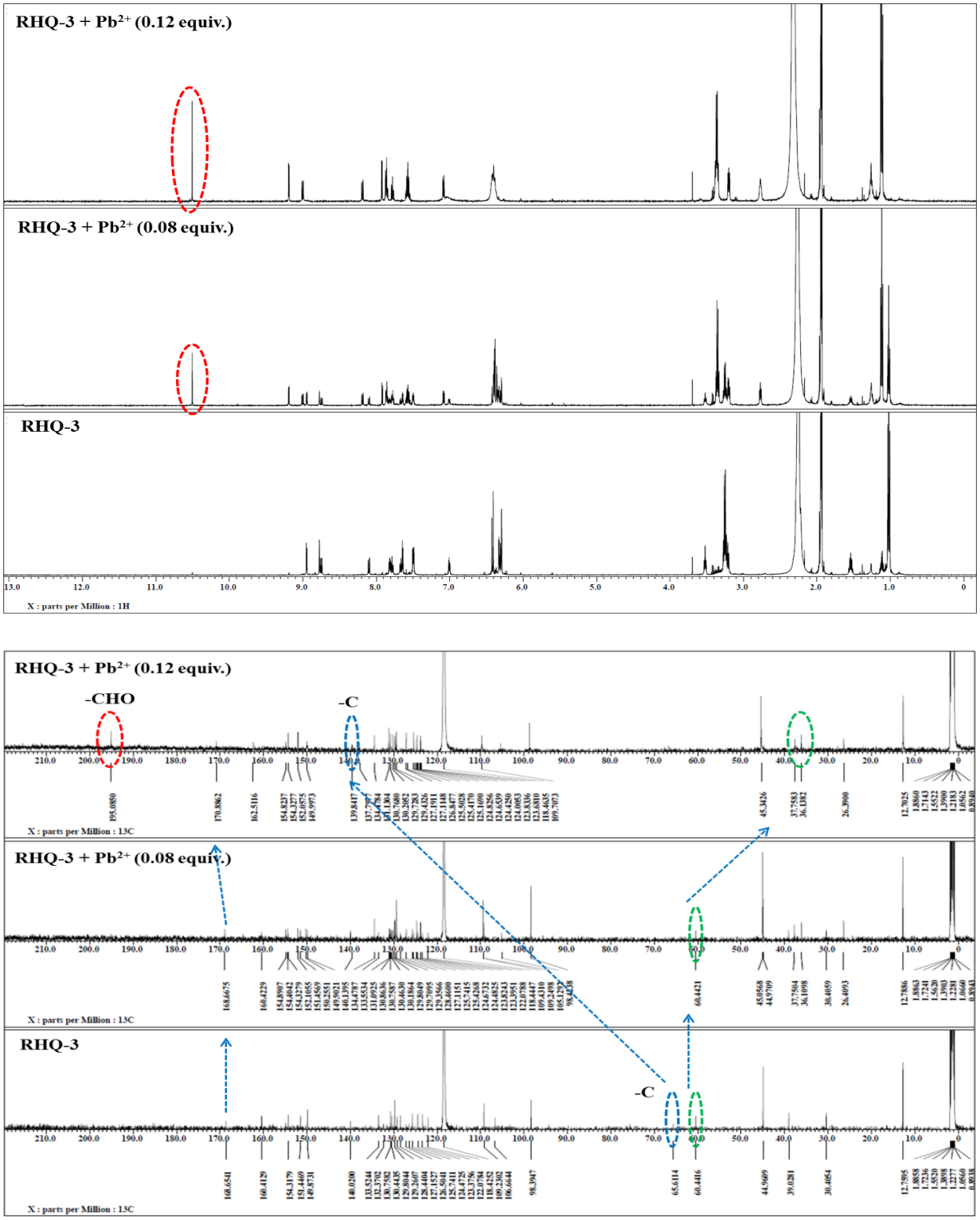

Fig. S44 ^{1}H NMR and ^{13}C NMR spectra of **RHQ-3** in CD_3CN-d_3 after addition of Pb^{2+}.

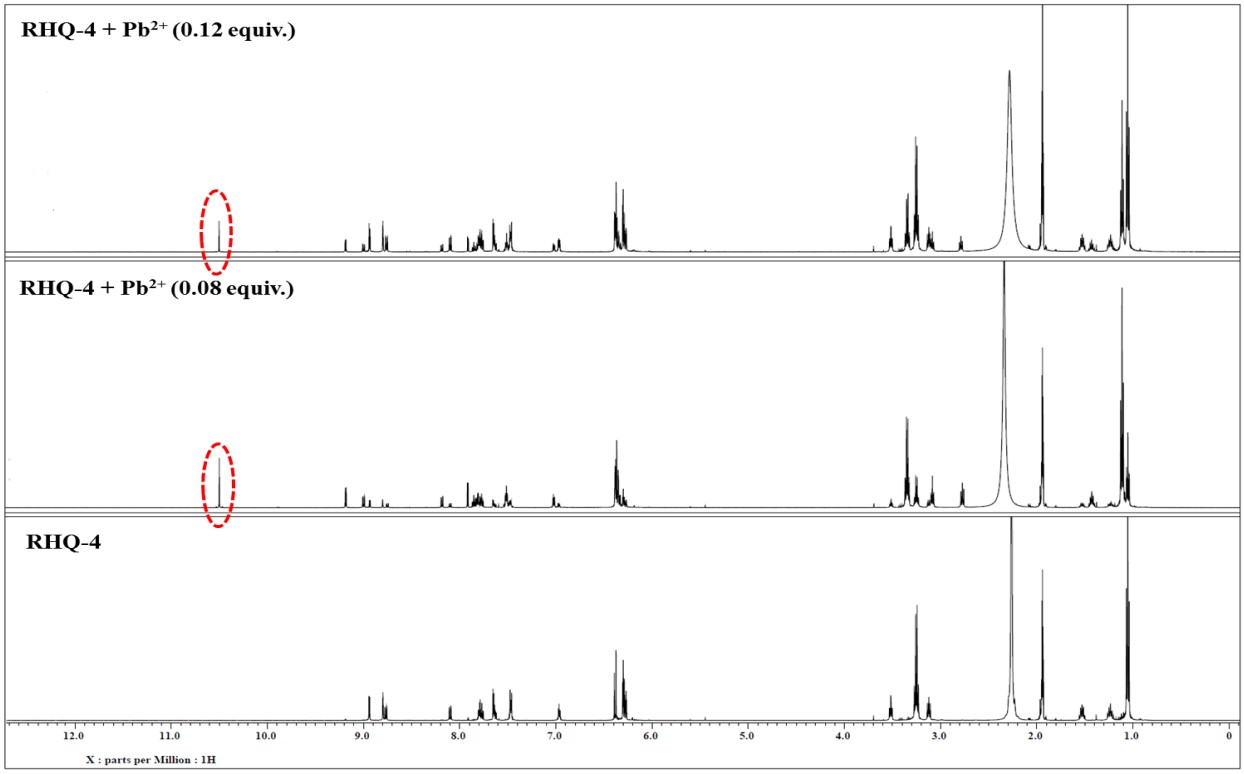

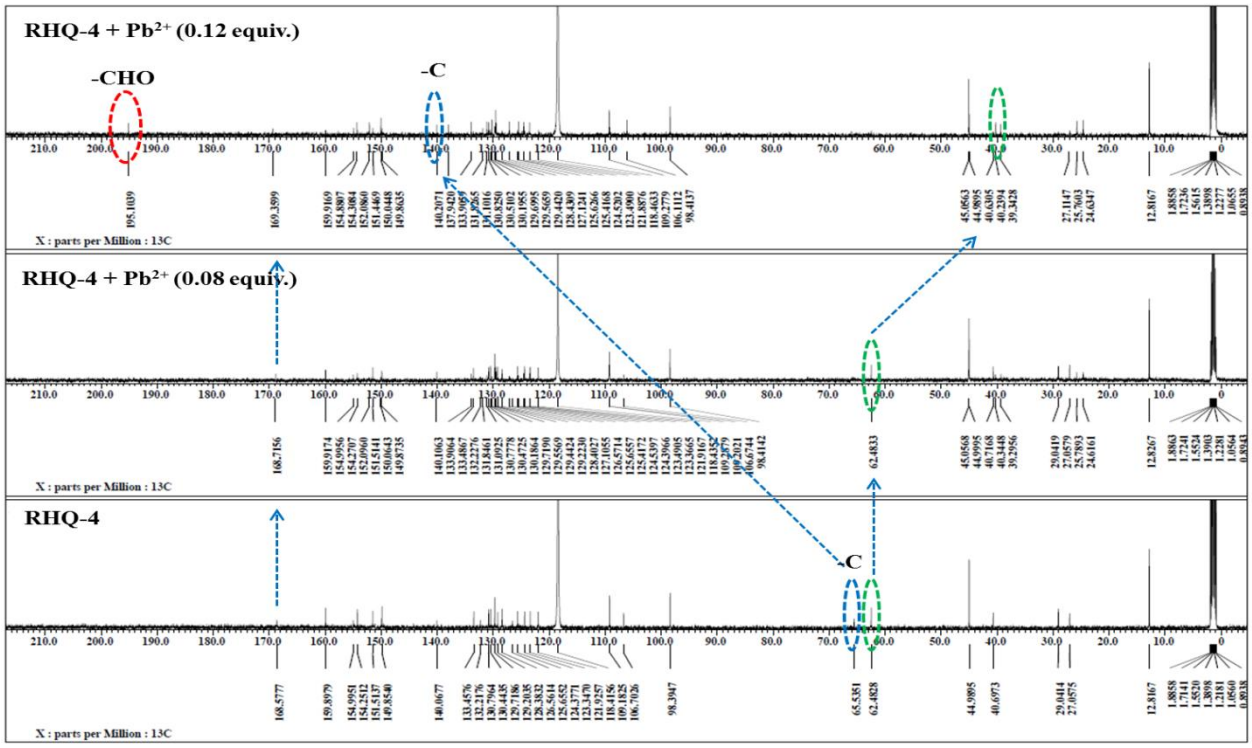

Fig. S45 ^{1}H NMR and ^{13}C NMR spectra of **RHQ-4** in CD_3CN-d_3 after addition of Pb^{2+}.

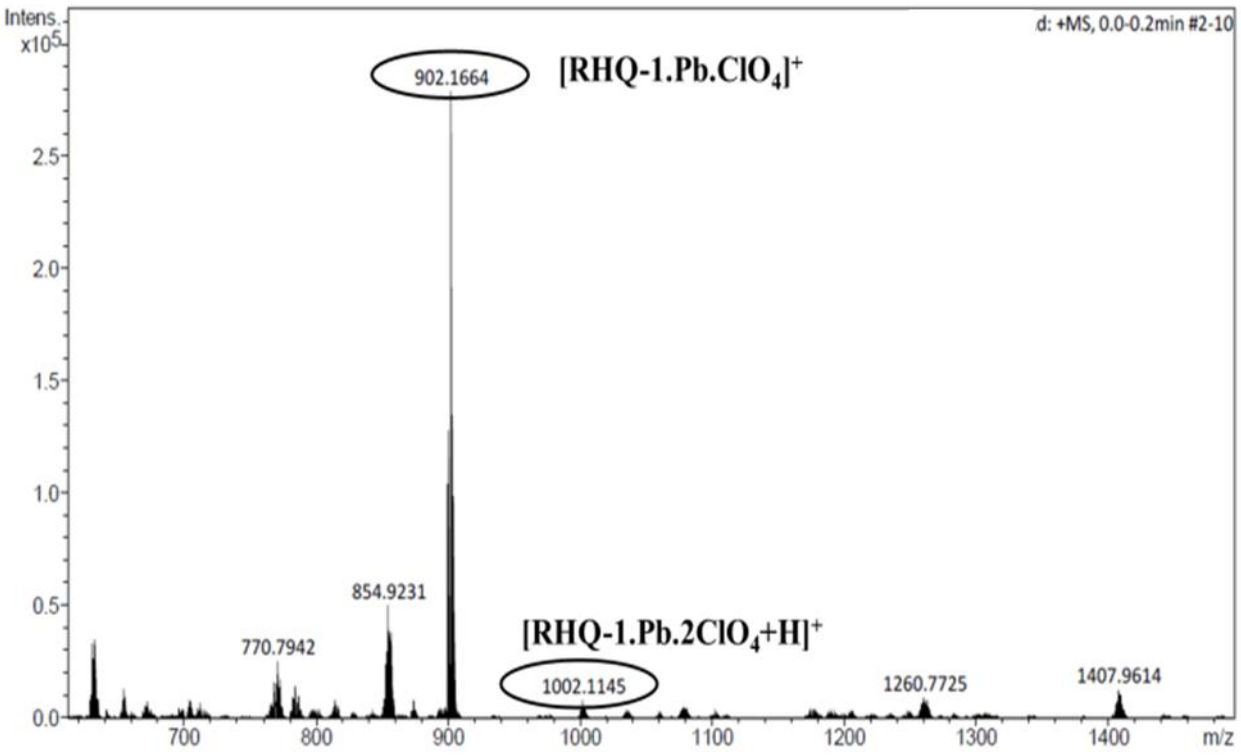

Fig. S46 Mass spectrum of **RHQ-1** in presence of Pb^{2+}.

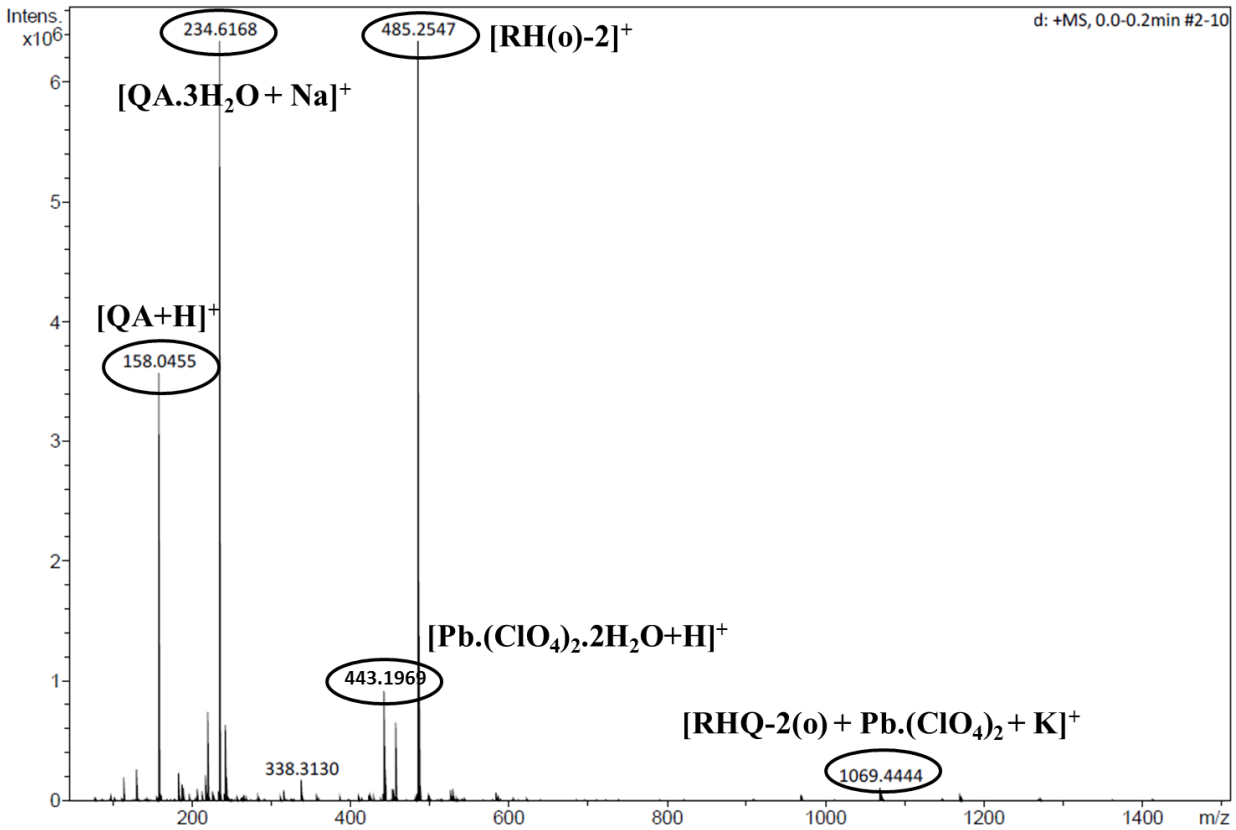

Fig. S47 Mass spectrum of **RHQ-2** in presence of Pb^{2+}.

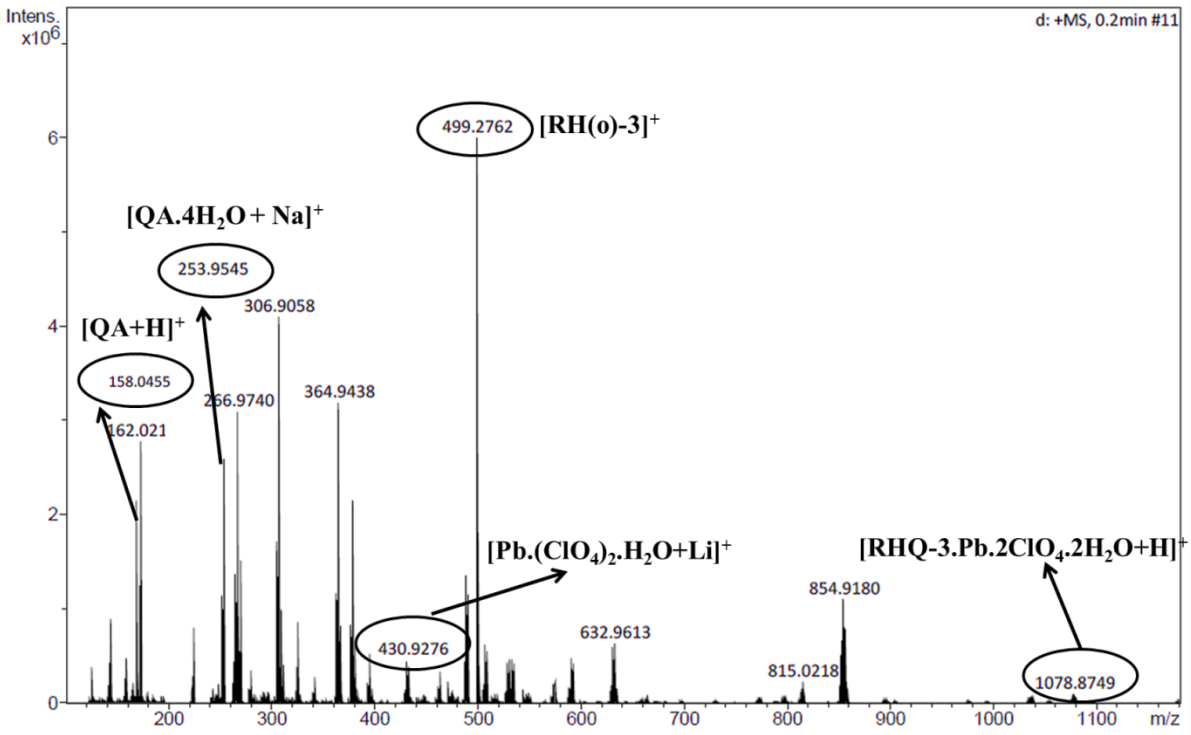

Fig. S48 Mass spectrum of **RHQ-3** in presence of Pb^{2+}.

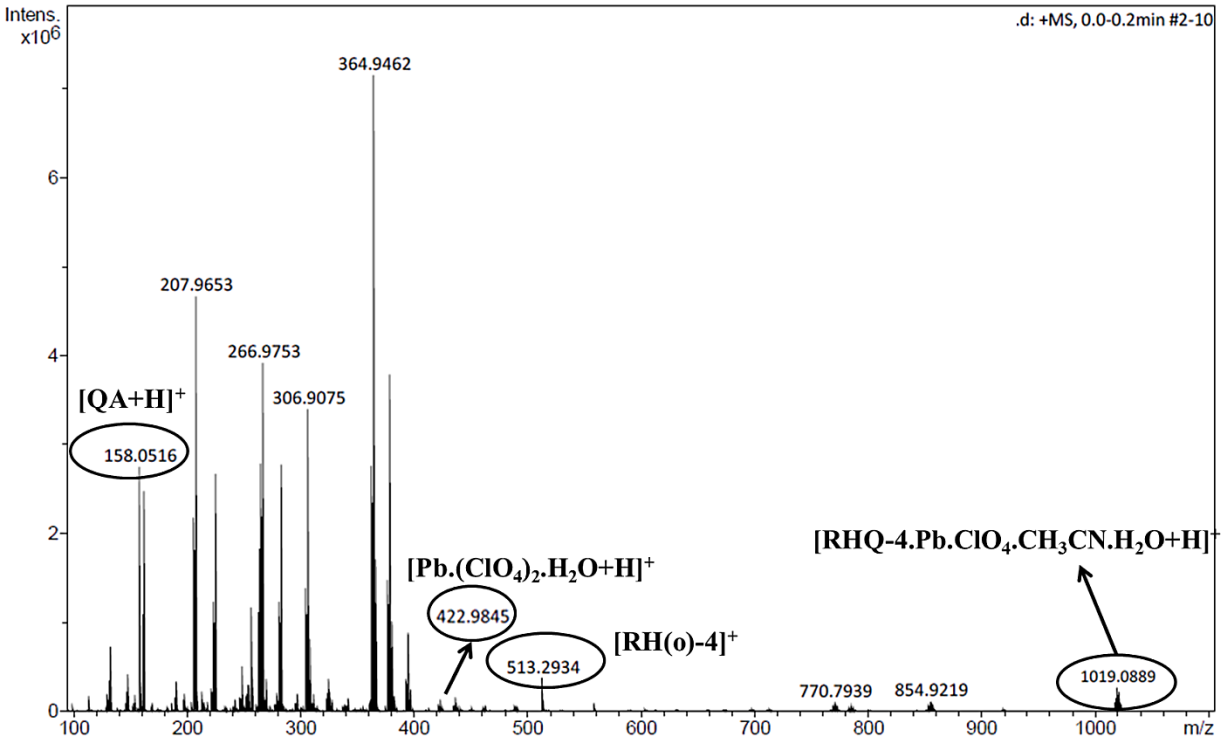

Fig. S49 Mass spectrum of **RHQ-4** in presence of Pb^{2+}.

Plausible mechanism of chemosensing

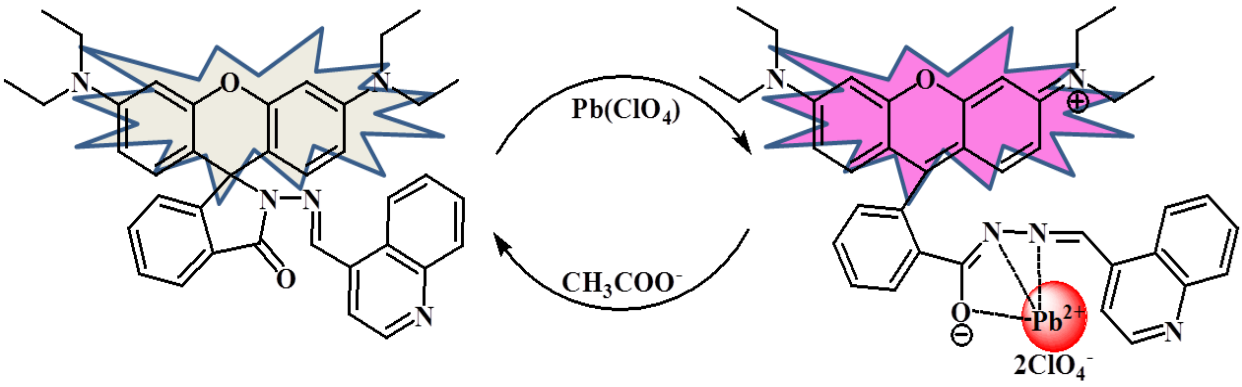

Scheme 1 Plausible mechanism of Pb^{2+} binding with **RHQ-1**.

Anion sensing

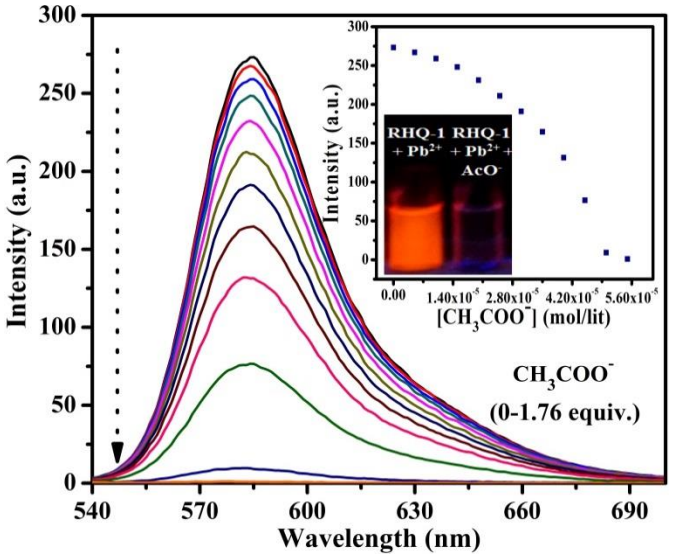

Fig. S50 Fluorescence spectra of **RHQ-1+Pb^{2+}** ensemble ensemble (1×10^{-5} M) upon addition of 0.061 equiv. of CH_3COO^- in CH_3CN:H_2O (9.5:0.5 %, *v*/*v*).

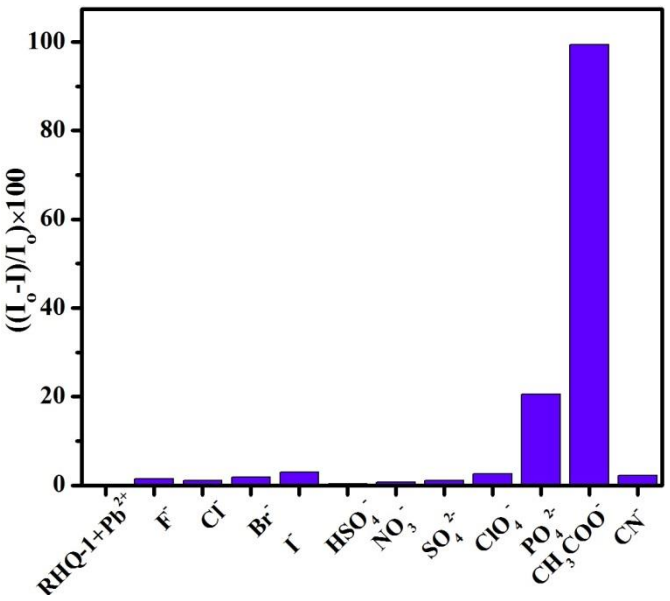

Fig. S51 Comparison of fluorescence intensity at 586 nm of **RHQ-1+Pb^{2+}** ensemble on addition of various anions. λ_{ex} = 530 nm.

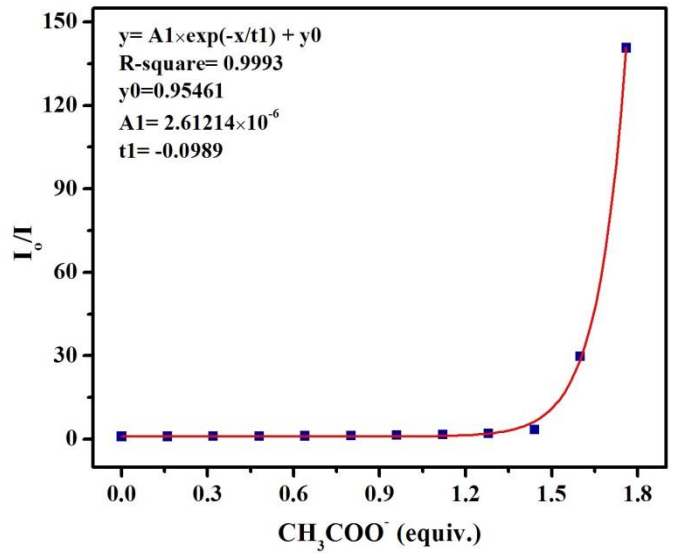

Fig. S52 Stern –Volmer plot of **RHQ-1+Pb^{2+}** ensemble on the addition of different amounts of CH_3COO^-.

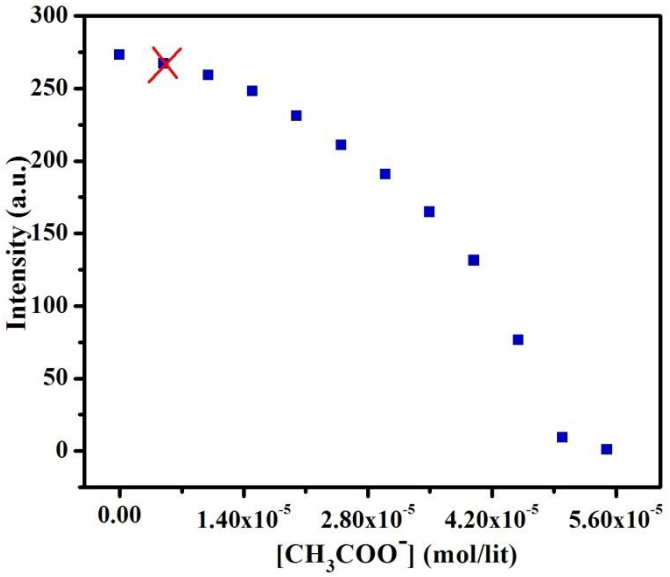

Fig. S53 Detection limit of **RHQ-1+ Pb^{2+}** ensemble for the detection of CH_3COO^-.

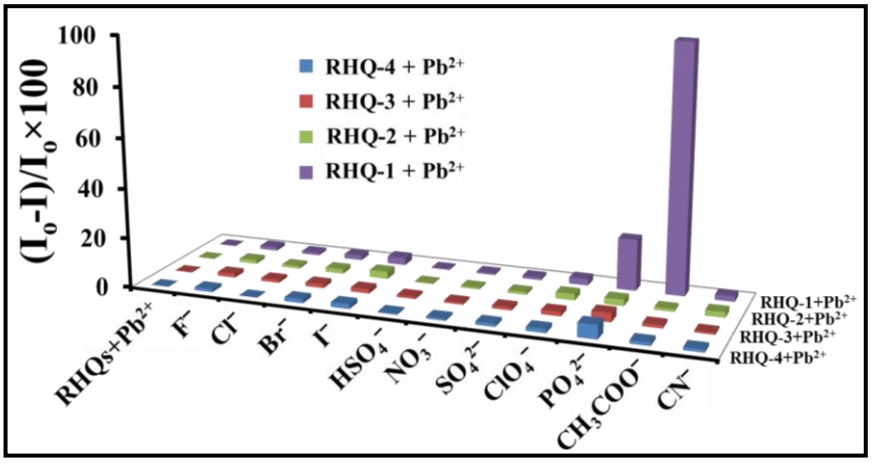

Fig. S54 Comparison of fluorescence intensity at 586 nm of **RHQs+Pb^{2+}** ensemble on addition of various anions, λ_{ex} = 530 nm.

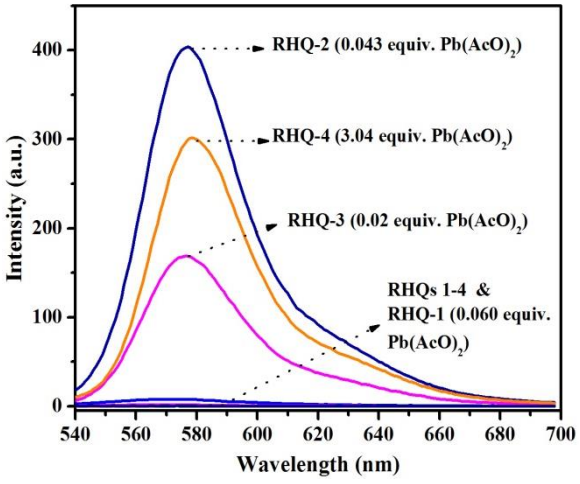

Fig. S55 Fluorescence spectra of **RHQs 1-4** (1×10^{-5} M) upon addition of 0.060, 0.043, 0.020 and 3.04 equiv. of $Pb(CH_3COO)_2$ in CH_3CN:H_2O (9.5:0.5 %, *v*/*v*) respectively.

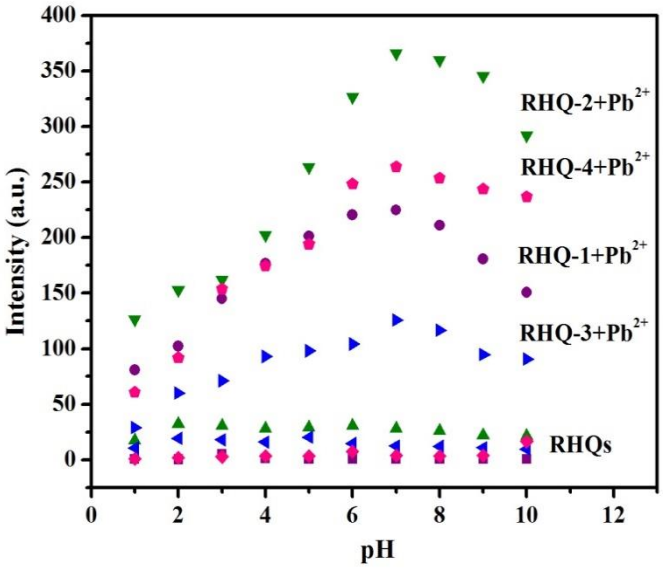

Fig. S56 Effect of pH on fluorescence intensity of **RHQs 1-4** (1×10^{-5}M) and **RHQs 1-4+Pb^{2+}** in Tris-HCl buffered (0.05M) solution.

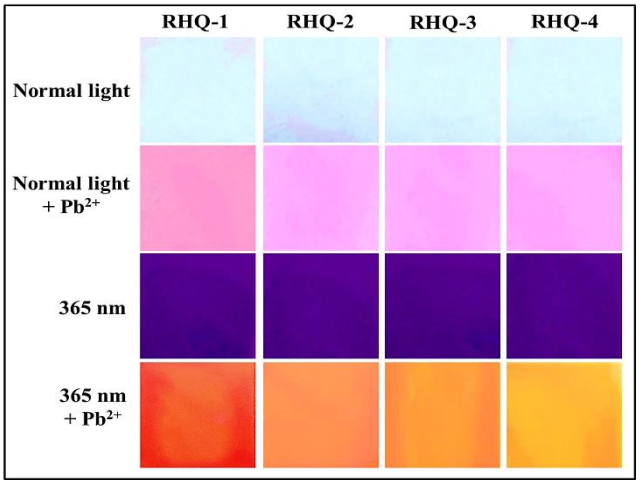

Fig. S57 (upper two rows): under normal light; (lower two rows) under UV light (365 nm). Test strips coated with **RHQs** viewed under normal light and 365 nm in abscence and prescence of Pb^{2+}.

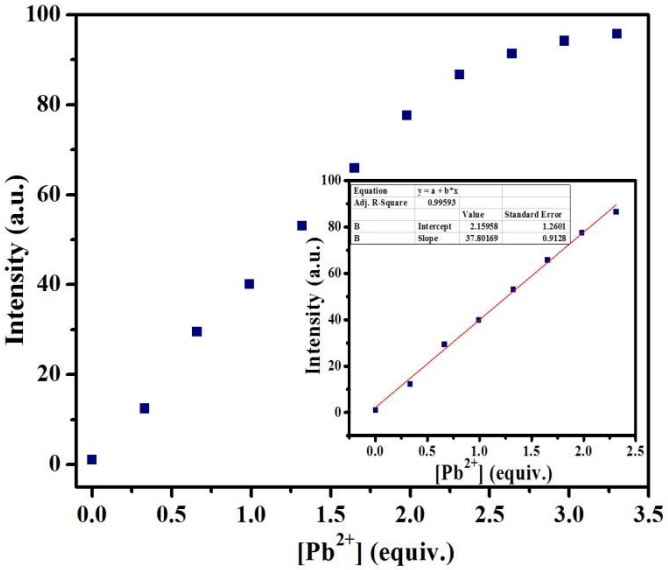

Fig. S58 Detection limit of **RHQ-1** (1×10^{-5} M) towards the detection of Pb^{2+} in tap water.

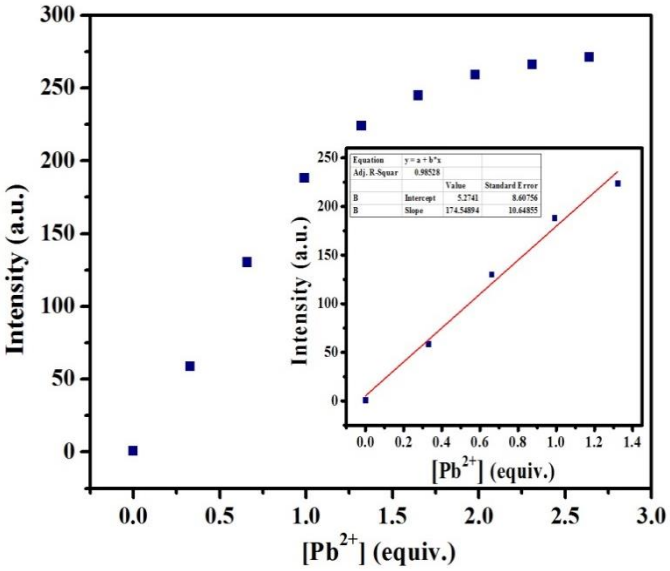

Fig. S59 Detection limit of **RHQ-2** (1×10^{-5} M) towards the detection of Pb^{2+} in tap water.

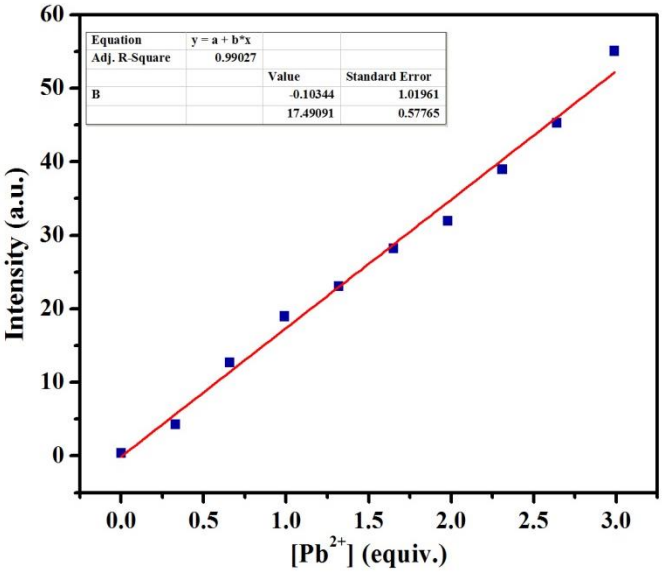

Fig. S60 Detection limit of **RHQ-3** (1×10^{-5} M) towards the detection of Pb^{2+} in tap water.

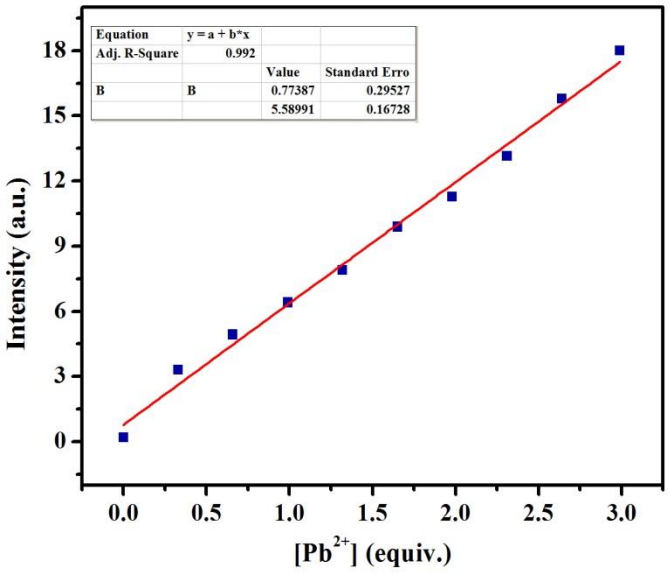

Fig. S61 Detection limit of **RHQ-4** (1×10^{-5} M) towards the detection of Pb^{2+} in tap water.

Comparison of detection limits

The detection limits of **RHQ-1, RHQ-2, RHQ-3** & **RHQ-4** towards Pb^{2+} in tap water were determined from the following equation:

$$DL=3•SD/S$$

Where SD is the standard deviation of the blank solution (**RHQ-1, RHQ-2, RHQ-3** & **RHQ-4**, 10 μM) detected for 10 times; S is the slope of the calibration curve.

S. No.	Standard Deviation	Slope	(3×Standard deviation)/Slope	Detection Limit	Detection Limit
1.	0.83	174.54894×10^{6}	0.0142×10^{-6}	1.42×10^{-8} M	14.2 nM
2.	0.74	37.80169×10^{6}	0.0587×10^{-6}	5.87×10^{-8} M	58.7 nM
3.	0.82	17.49091×10^{6}	0.1406×10^{-6}	1.40×10^{-7} M	0.14 μM
4.	0.80	5.58991×10^{6}	0.4293×10^{-6}	4.29×10^{-7} M	0.42 μM

Table S1. Comparison of **RHQs** with various reported rhodamine-based and other chemosensors for Pb^{2+}.

Derivative	**Solvent System**	**Sensing**	**Detection limit**	**Application For Pb^{2+} detection in Tap water**	**Reference**
Our system (RHQs 1-4)	ACN:H_2O	Pb^{2+}	17 nm, **6.91 nM**, 9.82 nM and 3 μM	**14.2 nM**, 58.7 nM, 0.14 μM and 0.42μM	**Present work**
RDP-1	HEPES	Pb^{2+}	15 nM		O. Sunnapu *et al.*, *RSC Adv.* **2016**, *6*, 656.
L	ACN:H_2O	Pb^{2+} Fluorimetric & Cu^{2+} colorimetric	Pb^{2+} (2.5×10^{-7} M) & Cu^{2+} (5.8×10^{-7} M)		M. Li *et al.*, *Dalton Trans.* **2015**, *44*, 17326.
Sensor 1	$CHCl_3$: THF	Pb^{2+}			L.-Q. Li *et al.*, *Spectrochemica Acta Part A: Molecular and Biomolecular Spectroscopy* **2014**, *122*, 722.
R1	MeOH:H_2O	Pb^{2+} (Absorbance in Tris-HCl) and Cd^{2+} (Fluorescence HEPES)			L. Xu *et al.*, *RSC Advances* **2012**, *2*, 6323.
Chemosensor 1	ACN	Pb^{2+}	10^{-4} M		H. Ju *et al.*, *Talanta* **2011**, *83*, 1359.
RPU	Mixed ACN:H_2O	Pb^{2+} & Hg^{2+}	7 nM and 35 nM		Zhi-Qiang *et al.*, *Chem. Commun.* **2010**, *46*, 3765.
LF1	HEPES	Pb^{2+}			Q. He *et al.*, *J. Am. Chem. Soc.* **2006**, *128*, 9316.
1	ACN	Pb^{2+}			J. Y. Kwon *et al.*, *J. Am. Chem. Soc.* **2005**, *127*, 10107.
Probe 1	H_2O:THF	Pb^{2+}	10 nM	Pb^{2+} using calibration method	A. Chatterjee *et al.*, *RSC Adv.*, 2014, **4**, 47076